ACS OMEGA

http://pubs.acs.org/journal/acsodf

Article

Further Studies on Cationic Gemini Amphiphiles as Carriers for Gene Delivery—The Effect of Linkers in the Structure and Other Factors Affecting the Transfection Efficacy of These Amphiphiles

Mange Ram Yadav,* Mukesh Kumar, and Prashant R. Murumkar

Cite This: *ACS Omega* 2021, 6, 33370−33388

Read Online

ACCESS | Metrics & More | Article Recommendations | Supporting Information

ABSTRACT: Gene therapy has the therapeutic potential to address a multitude of health problems, and it also has utility in different domains of science. However, its applications are plagued due to the absence of a suitable, safe, efficient, selective, and universal vector, which could help in delivering the desired nucleic acid cargo to the site of action. Though viral vectors are efficient, they pose various health risks. Different types of synthetic agents have been tried as nucleic acid vectors by researchers but with limited success. Gemini amphiphiles (GAs) are a class of synthetic surfactants having biscationic heads with attached hydrophilic and lipophilic groups. Herein, we synthesized two classes of GAs differing in the chemical nature and length of the linkers, head groups, and lipophilic chains. The resulting compounds were evaluated for their efficiency to transfect A549 and HeLa cell lines with a β-galactosidase reporter plasmid. A 3-oxypentyl linker, a monohydroxyethyl head group, and a tetradecyl moiety as the lipophilic chain offered the best transfection efficiency (compound **10BIII**). Dioleoylphosphatidylethanolamine (DOPE) as the helper lipid improved the transfection efficacy of the GAs in the absence of serum. In the presence of serum, DOPE and cholesterol, as the helper lipids, improved the transfection efficacy of the resulting formulations. The synthesized GAs showed concentration-dependent toxicity in the MTT assay. Biodistribution studies using ^{99m}Tc-labeled lipoplexes indicated that the lipoplexes got concentrated in some vital organs such as the spleen, liver, and lungs.

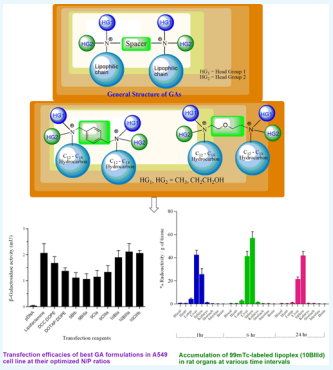

1. INTRODUCTION

Gene therapy has the potential to address hematological[1,2] and cardiovascular disorders,[3,4] neurological disorders,[5−8] cancers,[9,10] and genetic disorders. Advancements in this field have led to the approval of several nucleic acid tools[11] including small interfering RNAs,[12−14] antisense oligonucleotides,[15−21] and aptamers[22] by the Food and Drug administration (FDA). The very recent approval given in this field was mRNA-based vaccines against COVID-19.[23,24] Many diseases are caused by inheritance of defective or lack of particular genes. Initially, it was thought that such diseases could be treated by replacing the defective or missing gene with a normal copy of the gene through gene therapy. Later on, it was realized that many diseases are caused by dysregulation in expression of certain normal genes. Therefore, it was thought that such diseases could also be treated by implanting normally expressing genes from outside by gene therapy. Researchers have corrected defective or abnormal genes with normal genes through selectively controlling the expression of defective genes or their replacement.[25]

The two basic requirements of gene therapy are (i) a suitable therapeutic gene/nucleic acid that could be expressed at the target site[26] and (ii) a delivery system that is safe and effective for the delivery of the therapeutic gene(s) to the targeted tissue or organ.[27] In theory, it seems to be very simple and straightforward, but it poses enormous problems when put to practical applications. The major problem in gene therapy is safe delivery of the desired gene(s) into the targeted tissue, where it could show its expression. Since 1989 when the first clinical trial in human gene therapy was performed, innumerable clinical trials have been carried out/approved, but the core issue of finding a suitable and efficient system for delivering the gene at the target site has not been fully resolved as yet.[28] The development of vectors capable of addressing all the issues related to gene delivery could make gene therapy a general method of treatment for many diseases. Because gene delivery is a multistep process in which an appropriate property of the carrier would be needed to carry forward each step at the molecular level, rationally designed multifunctional vectors could overcome various extra- and intracellular barriers.[29] A wide spectrum of gene delivery systems has been developed in order to overcome these barriers involving different aspects of ligand conjugation chemistry, DNA condensation technology,

Received: July 12, 2021
Accepted: September 30, 2021
Published: December 1, 2021

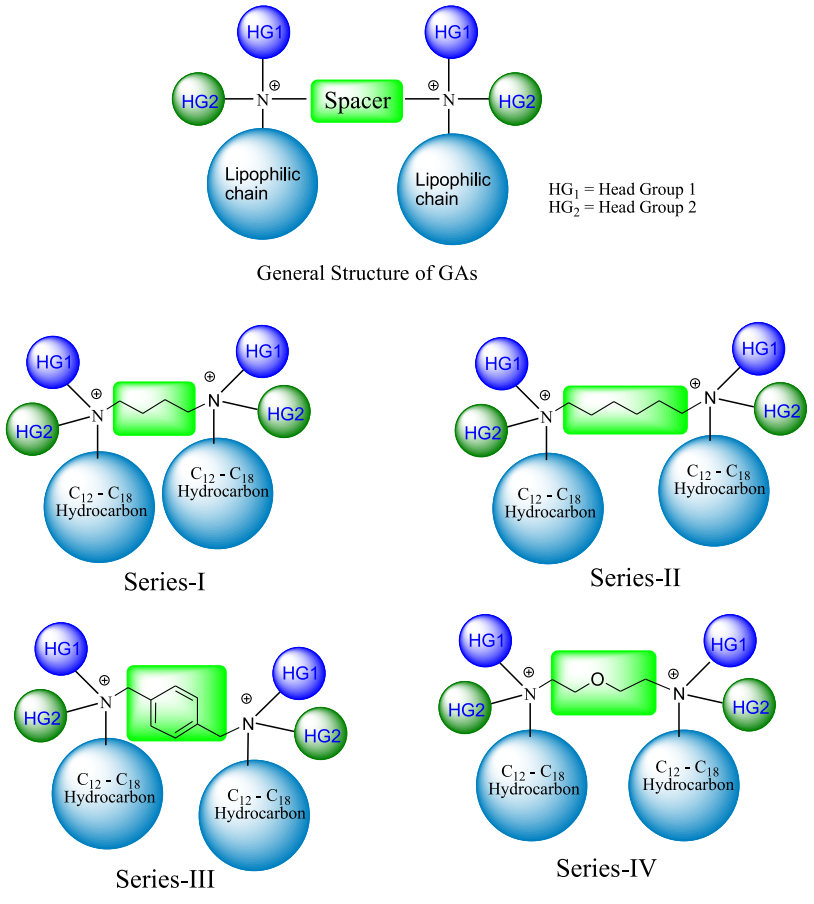

Figure 1. General structure of the designed GAs (Series-III and IV).

and molecular biology. Therefore, for successful gene therapy, a safe, selective, and efficient vector, an appropriate delivery technique, and a suitable nucleic acid cargo are the prerequisites.

Naked DNA being a hydrophilic, polyanionic, long, and slender molecule having micrometer dimensions encounters a number of barriers when administered all alone, restricting its cell permeability.[30] Colloidal instability, RES uptake, and difficulty in organ and cellular targeting are the other major problems posing a big challenge to the delivery of naked nucleic acids.[31] Naked nucleic acid gets degraded by serum nucleases when administered intravenously. This degradation can be partially resolved by combining the nucleic acid with a cationic lipid/polymer/inorganic material capable of complexing with it or entrapping it by ionic interactions. A number of carriers/vectors have been developed to address the aforementioned problems associated with the delivery of naked nucleic acids. Therefore, suitable delivery systems are required to fulfill the delivery requirements of nucleic acids. Use of viruses for gene delivery could induce a measurable effect even with the introduction of a single viral particle, but there are certain limitations such as the possibility of oncogenicity, mutagenicity, immunogenicity, resistant to transfect the non-dividing cells, rejection by the host cells, or limited DNA cargo-carrying capacity while using viral vectors.[32−35] Due to these problems, there is a dire need for the development of non-viral systems for the delivery of genetic materials to the host.

Unlike small molecules, DNA cannot diffuse easily into the nucleus from the cytoplasm. Therefore, a carrier system plays a vital role not only in the endocytosis of the DNA cargo but also in its intracellular trafficking and transcription of the genetic material in the nucleus. The carrier can either condense with DNA or encapsulate DNA into its polymeric matrix. Cationic polymers used as carriers form complexes with DNA due to charge−charge interactions to offer polyplexes.[36] Normally, these carrier systems containing a hydrophilic head and a hydrophobic tail exhibit surface-active properties. These carrier systems are used for multifarious applications including their use in gene delivery systems.[37] The cationic lipid carriers help the negatively charged DNA in penetration through the cell membrane, protect the bound DNA cargo against deoxyribonuclease (DNase) degradation, and in transfecting the cells with the nucleic acid material. Transfection efficacy of a carrier is governed by its overall structure and the presence of positive charge on its surface. A carrier molecule should possess optimal hydrophobicity as well as hydrophilicity. Therefore, a carrier molecule can have variations in the chemical nature and length of the spacer, the lipophilic hydrocarbon chain, and the hydrophilic head group. Therefore, the use of modular structures of the carriers/vectors is an ideal concept in the design of nucleic acid carriers. For a carrier having a modular structure, changes in its transfection efficiency can easily be studied by varying the chain length of the hydrophobic group, the size and type of linkers, or the type of head groups, and suitable changes in the

https://doi.org/10.1021/acsomega.1c03667
ACS Omega 2021, 6, 33370−33388

Scheme 1. Synthesis of the Final Compounds (9AI, 9BI−9BIV, 9CI−9CIV, 10AI, 10BI−10BIV and 10CIII, and 10CIV)

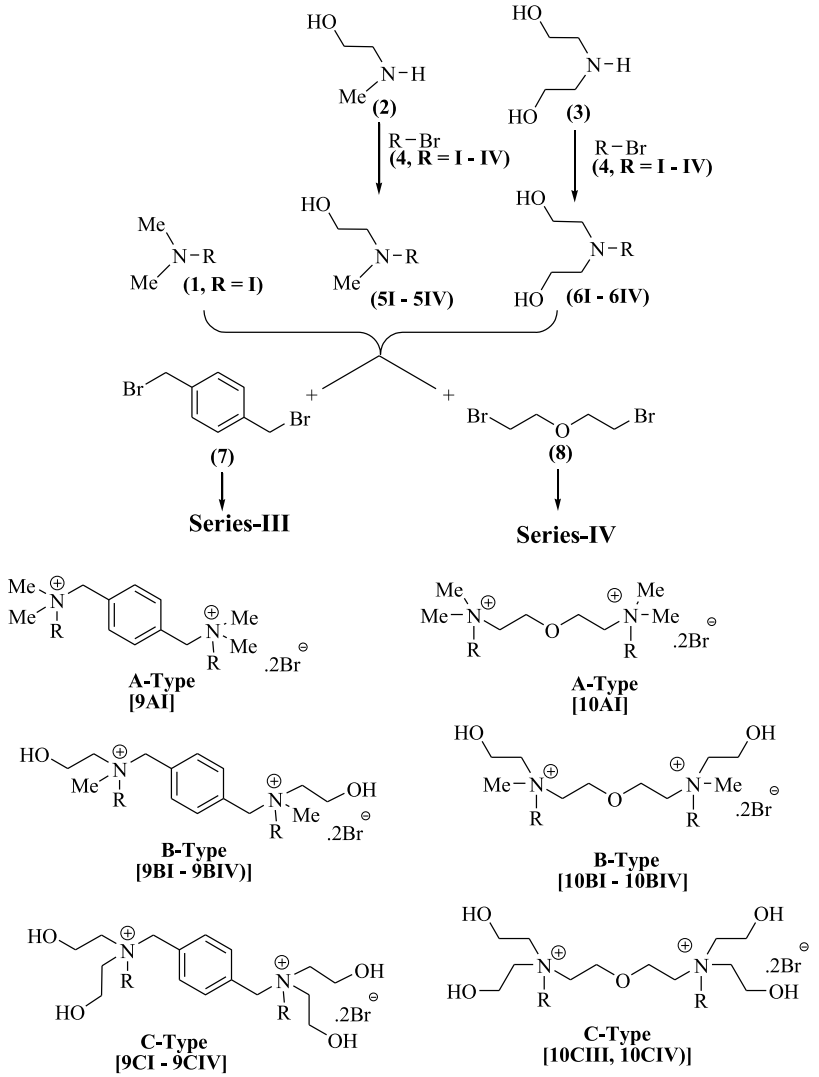

modular structure of the carrier could easily be effected as per the need.

Gemini amphiphiles (GAs) are a class of positively charged divalent synthetic surfactants designed for the delivery of nucleic acids. GAs have two cationic heads having a lipophilic chain attached to each one of them, and the two cationic heads are joined together through a linker/spacer. These GAs form liposomes when formulated all alone or along with helper lipids above their transition temperatures. When combined with DNA, they cause condensation and size reduction of the DNA molecules offering small particulate structures (i.e., lipoplexes), which protect the DNA from degradation by DNases. GAs as synthetic carriers are of interest for the delivery of genetic materials due to their unique physicochemical properties. GAs,[38] in particular, and polymeric agents,[39] in general, have been reviewed recently.

Transfection efficacy is a function of many factors such as the structure of the GAs having different hydrophobic groups, head groups, and spacers,[40,41] use of different types of helper lipids to prepare liposomes, the ratio of the GA to DNA concentration (i.e., the N/P ratio), size and zeta potential of the lipoplexes, and the type of cell lines used for their in vitro evaluation. Serine-based cationic gemini surfactants with different alkyl chain lengths, and amine/amide or ester groups as spacers/linkers offered good binding to the DNA molecules with efficient in vitro transfection property and high cell viability. However, the nature of the spacers linking the two head groups markedly influenced the DNA release from the polyplexes, with spacers having ester groups being the least efficient.[42] Gemini surfactants having hexadecyl tails and hydroxyethylated head groups abridged with longer carbon-chain spacers yielded the maximum transfection efficacy.[43]

Earlier, we reported[44] two series of GAs (Series-I and Series-II) in which the spacers between the two cationic heads were C_4 and C_6 chain hydrocarbons (Figure 1). In this paper, we report two more series of GAs (Series-III and Series-IV), in which the chemical nature of the spacer was changed from a hydrocarbon to aromatic system and a hydrophilic chain with a slight variation in the interonium distance between the two

https://doi.org/10.1021/acsomega.1c03667
ACS Omega 2021, 6, 33370−33388

cationic centers while maintaining the head groups and the lipophilic tails.

In our previous report, we have reported[42] that moving from the $(CH_2)_4$ to $(CH_2)_6$ spacer caused a marked decrease in transfection efficacies of all of the GA formulations. Two major changes were carried out in the spacers in this report. In one series (Series-III), an aromatic ring was introduced in place of a straight chain hydrocarbon with interonium distance in between a tetramethylene and hexamethylene, while in the other one (Series-IV) a polar oxygen function was introduced along with a carbon chain length in between $(CH_2)_4$ and $(CH_2)_6$. The basic idea behind these modifications was to see the impact of these changes in the spacers on the transfection efficacies of the resulting GAs. Attaching two hydroxyethyl groups to the hydrophilic head in place of one also caused a slight decrease in the transfection efficacies, while the order of the lipophilic hydrocarbon chain was $C_{14} \approx C_{16} > C_{18} > C_{12}$ with tetradecyl and hexadecyl chains offering the best results.[44] Considering the outcome of these reports,[42,44] the head groups and the hydrophilic chains were retained as such in the newly synthesized GAs with one difference, that is, the number of synthesized GAs having only dimethyl or di(2-hydroxyethyl) head groups, and C_{12} or C_{18} lipophilic tails were reduced as these were found not to offer GAs having good transfection efficacy in our earlier report.[44]

It was planned to evaluate the effects of changes in the ratio of the GA to nucleic acid, and the effects of other additives on the transfection efficacy of the synthesized GAs and cell toxicity of the synthesized GAs. Impacts of various formulation parameters like incorporation of helper lipids such as dioleoylphosphatidylethanolamine (DOPE) or cholesterol in the formulation on the transfection efficacy of the GAs was also planned to be studied.

2. RESULTS AND DISCUSSION

2.1. Chemistry. Two main series of GAs were synthesized with variations in the type and size of spacers/linkers. In one series, the two cationic heads were joined by a *p*-xylyl linker (Series-III), while in the second series a polar linker 3-oxypentyl (Series-IV) with a different chain length was used. In each main series, compounds belonging to three subseries were prepared by varying the polarity of the cationic heads by replacing one or both of the methyl groups of dimethylamine (A-Type) by a monohydroxyethyl (B-Type) or a di-(hydroxyethyl) (C-Type) group. The lipophilic chains in each subseries were varied from the original $C_{16}H_{33}$ (**I**) to $C_{12}H_{25}$ (**II**)/$C_{14}H_{29}$ (**III**) or $C_{18}H_{37}$ (**IV**) hydrocarbons to obtain the final compounds (**9AI**, **9BI**−**9BIV**, **9CI**−**9CIV**, **10AI**, **10BI**−**10BIV** and **10CIII**, and **10CIV**).

For the synthesis of the final compounds, the tertiary amines (**1**, **5I**−**5IV**, or **6I**−**6IV**) were reacted either with *p*-dibromoxylene (**7**) or with di(2-bromoethyl)ether (**8**) to obtain the desired GAs [**9AI**−**10CIV**]. All of the tertiary amines except for hexadecyldimethylamine (**1**) were prepared by reacting the desired secondary amines (**2** or **3**) with suitable bromo derivatives (**4I**−**4IV**) of the hydrocarbons of the required chain lengths (**I**−**IV**) as depicted in Scheme 1. Compounds of three subseries (Types-A, -B, and -C) were prepared, with differences in the structures of the head groups in each series (Series-III and Series-IV). The synthesized compounds are in conformity to their assigned structures. The structures of the synthesized compounds were confirmed on the basis of their elemental analyses and proton NMR (PMR) spectroscopy data. In compounds of Series-III, the four aromatic protons appeared at δ 7.4−7.8. Protons of the hydrocarbon chains offered characteristic signals for the terminal methyl groups at around δ 0.85. Three additional characteristic signals could also be identified for the hydrocarbon chains; one for the methylene attached to the quaternary nitrogen atoms, second for the adjoining methylene group of the hydrocarbon chains, and the third for the remaining methylene groups, which appeared as a broad signal at δ 1.25−1.85. The chemical shift values for the methylene attached to the quaternary nitrogen and the adjoining methylene of the hydrocarbon chain varied depending on the nature of the head groups and the spacer. Methylenes of the *p*-xylyl group appeared at δ 5.26 in compound (**9AI**) but in monohydroxyethyl and di(hydroxyethyl) derivatives (**9BI**-**9BIV** and **10CI**−**10CIV**), this signal got bifurcated and appeared at different values of chemical shifts. The position of the hydroxyl protons in the subseries (Types-B and -C) also did not appear at a fixed δ value. Signals appearing for the methylenes of the diethyleneoxy group present as a spacer (in Series-IV) and of the hydroxyethyl/di(hydroxyethyl) groups (Series-III and Series-IV) could not be assigned unambiguously on the basis of the existing data. However, the integration values for the total number of protons in all the synthesized compounds matched exactly with the stipulated structures. Elemental analyses of the synthesized compounds confirmed the final structures.

2.2. Formulation Aspects of the Synthesized GAs. *2.2.1. Critical Micelle Concentration Determination of the GAs.* In order to evaluate the surfactant properties of the synthesized GAs, their critical micelle concentration (cmc) was determined using conductometry.[45] This method is based on the fact that conductance of the amphiphiles changes at different rates below and above the cmc. This difference in aggregation behavior is controlled by co-operativity of both inter- and intramolecular interactions of GAs, besides their interactions with solvents. At low concentrations, the amphiphiles dissociate and ionize completely. At concentrations below cmc, their conductance increases linearly, while above the cmc the amphiphile molecules start associating with one another to generate micelles. This leads to a change in the rate of increase in the conductance above cmc. The cmc values were obtained by using break points in concentration versus specific conductance plots. A representative plot for cmc determination is shown in Figure S1 and the results are compiled in Table 1S.

The surface-active properties of the synthesized GAs were observed to be much superior in comparison to their monomeric counterparts. For instance, **10BIV**, **10BI**, and **10CIV** showed cmc values of 1.0×10^{-6}, 1.3×10^{-6}, and 1.3×10^{-6} M, respectively. These cmc values were found to be 1000-fold lower than that of the monomeric surfactant, CTAB (1.3×10^{-3} M).[46] Comparison of the cmc values of GAs showed that as the polarity of the head group increased due to the incorporation of hydroxyethyl groups, the cmc values of the GAs decreased. The results obtained are suggestive of much better surfactant properties of the GAs having polar head groups compared to the GAs having non-polar head groups.

2.2.2. Liposomal Formulations of the Synthesized GAs. All the synthesized GAs were formulated as liposomes either alone [Plain Formulation] or with DOPE as a helper lipid in molar ratios (GA/DOPE) of 1:1 [Formulation (a)], 1:2 [Formulation (b)], and 1:3 [Formulation (c)]. Effective fusogenic

https://doi.org/10.1021/acsomega.1c03667
ACS Omega 2021, 6, 33370−33388

properties at the endosomal stage possessed by DOPE were instrumental in using DOPE as the helper lipid.[47] The pH of the solution was maintained at 7.4 using a buffer system containing 4-(2-hydroxyethyl)-1-piperazineethanesulfonic acid (HEPES) (20 mM). HEPES does not cause any hindrance in offering DNA lipoplexes because it is non-ionic in nature. A blend of solvents (chloroform/methanol, 1:1) was used to dissolve the GAs with or without the helper lipid. Cholesterol was also used as a helper lipid along with DOPE in some other formulations [formulations (d and e); compositions of formulations (d and e) are defined in later sections] to improve the formulation characteristics for some studies.

Almost all GAs exhibited a bimodular size distribution (two peaks in their size distribution report). The results reported here are the average size (*Z*-average) for all the analysis. The results of plain formulations of **9AI**, **9BI**, and **9CI** are shown in Table 1. All these formulations showed positive zeta potential

Table 1. Size and Zeta Potential of Plain Liposomes

liposomal plain formulation	size Z_{av}, nm (PDI)	zeta potential (mV)
9AI	326 (0.532)	30.1
9BI	370 (0.698)	48.9
9CI	400 (0.483)	46.4

(ZP) due to the presence of quaternary nitrogens in their structures, which is a necessary requirement for complexation with anionic plasmid DNA (pDNA). Relatively higher values of the polydispersibility index (PDI) were obtained due to the bimodular size distribution in the formulations. It may be due to free GA molecules along with their aggregates. The results showed that as the polarity of the head group increased in the GAs from **9AI** to **9BI** to **9CI**, the *Z*-average (Z_{av}) increased from 326 to 370 to 400 nm, while the hydrophobic chain length was kept constant. This may be due to an increasing propensity of the head group to hydrate with increasing number of hydroxyethylated groups.

The method of preparation also had a significant effect on Z_{av} of the formulations. For instance, formulation of **9BI** showed Z_{av} and PDI of 725 nm and 0.802, respectively, before sonication. DOPE incorporation into the formulation also caused an increase in Z_{av}.

2.2.3. Formulation of Lipoplexes with the Reporter DNA and Their Characterization. pDNA was incorporated using different N/P ratios (0.25 to 6) of the GA to obtain lipoplexes. The N/P ratio is defined by the ratio of nitrogen contents (of the GA) to the phosphorus contents (of pDNA). The quantity of the pDNA was kept constant and the quantity of the GA was varied while formulating the lipoplexes. pDNA dilutions and the volume of the cationic liposomal formulations were kept constant in the lipoplex formulations. The particle size of the prepared lipoplexes was found to depend on the incubation time after mixing of the GA formulation and pDNA. Lipoplexes of the pDNA were also prepared using the standard transfection reagents such as 1,2-dioleoyl-3-trimethylammonium-propane (DOTAP)−DOPE, *DCC−DOPE, or Lipofectamine for the purpose of performing comparative studies (*DCC: 3-[*N*-(*N*′,*N*′-dimethylaminoethane)carbamoyl]-cholesterol hydrochloride).

The Z_{av} and ZP values were also determined for the lipoplexes of formulations that showed the best results under transfection studies (e.g., **10BIIIa** given in Table 2 as a representative one). The blank (without pDNA) formulation

Table 2. Size and Zeta Potential of the 10BIIIa Lipoplex

formulation	N/P ratio	size, Z_{av} in nm (PDI)	zeta potential in mV
10BIIIa blank liposomes		214 (0.461)	29.6
Lipoplex of **10BIIIa**with pDNA	0.25	486 (0.725)	−14.9
	0.5	477 (0.313)	−9.08
	1.0	318 (0.348)	−2.98
	1.5	241 (0.266)	1.16
	2.0	222 (0.287)	2.91
	2.5	278 (0.315)	3.36
	3.0	290 (0.385)	6.83
	3.5	293 (0.291)	15.0
	4.0	345 (0.387)	16.9

of **10BIIIa** showed Z_{av} and ZP of 214 nm and 29.6 mV, respectively. However, its lipoplex with pDNA showed different values for Z_{av} and ZP depending upon the N/P ratio. At the lowest N/P ratio (0.25), the polyplex showed Z_{av} and ZP of 486 nm and −14.9 mV, respectively. With increasing N/P, the size of lipoplexes first decreased and then increased; while an increase in the N/P ratio (from 0.25 to 4.0) caused an increase in the ZP (−14.9 to 16.9 mV).

Transmission electron microscopy (TEM) photograph of the lipoplex of **10BIIIa** at its optimized N/P ratio is shown in Figure 2. The results obtained in the TEM study were in consonance with those obtained with DLS.

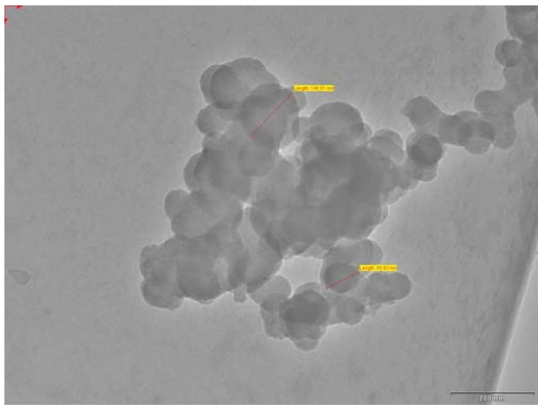

Figure 2. TEM image of the **10BIIIa** lipoplex at its optimized N/P ratio (N/P2); scale bar is equivalent to 240 nm.

2.3. Agarose Gel Retardation Assay for pDNA Complexation. Complex formation between the positively charged GA and the negatively charged pDNA was verified by agarose gel retardation assay. Ionic interactions between the two oppositely charged species would offer a neutral complex, which would not move on the electrophoretic gel under the influence of the applied voltage and would reside inside the well. However, the uncomplexed pDNA would migrate away from the well under the influence of the applied voltage.[48]

A representative gel electrophoretic pattern for lipoplex formulation of GA (**10BIIIa**) has been shown in Figure 3. Lane 1 shows plain pDNA (without complexing with GA), which has migrated out of the well with the application of external voltage. However, pDNA in other lanes gets retarded depending on the degree of the N/P ratio. With an increase in the N/P ratio from 0.25 to 3.0, there is a higher retention of pDNA with increasing value of N/P. All GAs showed ∼60%

https://doi.org/10.1021/acsomega.1c03667
ACS Omega 2021, 6, 33370−33388

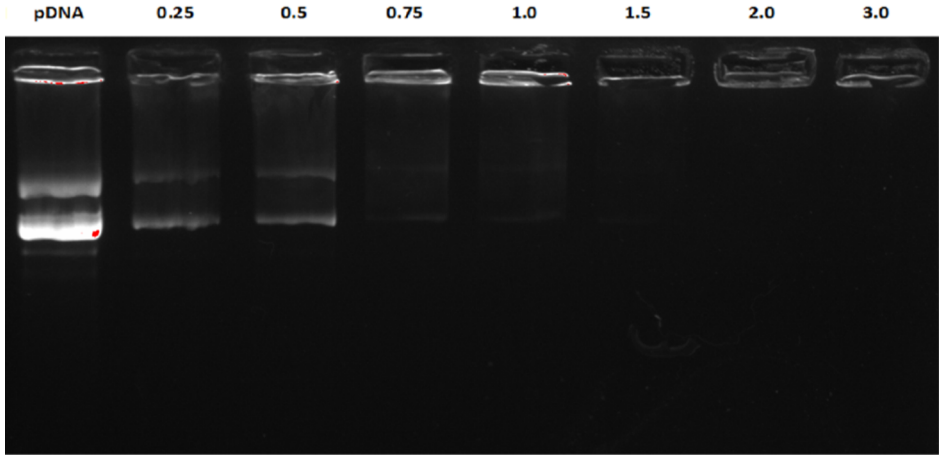

Figure 3. N/P complexation behavior of the synthesized GA (**10BIIIa**) under gel electrophoresis. Lane 1 (pDNA all alone), and lanes 2 to 8 [pDNA with GA (N/P 0.25 to 3.0)].

retardation at a N/P ratio of 0.5. At a N/P ratio of 1.0 and higher, 100% pDNA retention has been observed in the wells for all the GAs. Even at a 0.25 N/P ratio, a substantial amount of pDNA got retained in the well. Head group polarity, nature of linker, or the hydrophobic chain length of the GAs were found to be inert in influencing the migration of pDNA in this study as all the GAs showed almost similar retardation patterns at similar N/P ratios.

2.4. DNase I Digestion Study. The pDNA digestion study was used to evaluate the pDNA-protecting ability of the synthesized GAs against DNases. A nucleic acid vector used in the delivery system should provide protection to the genetic cargo against the invading DNases. The results obtained in the study showed that GAs in the N/P ratio of 1 or more than 1 caused complete protection of the pDNA against the action of DNase I. Representative graph for the GA formulation (**10BIIIa**) is shown in Figure 4. pDNA is shown in Lane 1,

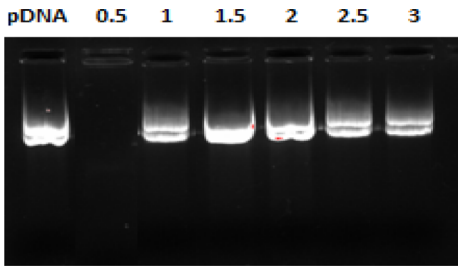

Figure 4. DNase digestion study to evaluate pDNA protection by various ratios of the GA (**10BIIIa**) present in the lipoplex.

which was not given DNase I treatment. In Lane 2, complete degradation of pDNA has taken place at a N/P ratio of 0.5. However, at N/P 1, approx. 90% of pDNA could be protected by the GA formulation. Full protection of pDNA against DNase I was observed at a N/P ratio of 1 and higher. Changes in the structures of the head group, linker, or hydrophobic chain of the GAs did not show any impact in this study also.

2.5. Circular Dichroism Study of pDNA Condensation. For obtaining high transfection efficacy, the nucleic acid cargo must remain undamaged.[49,50] Simberg et al. demonstrated that the formation of the compact form of DNA (i.e., ψ-DNA) is necessary for efficient gene delivery.[51] A compact form of DNA helps in its penetration into the cell. Complexation of the DNA with the vector should lead to the formation of a compact polyplex structure due to the reduction in the size of the DNA that helps not only in its penetration into the cell but also protects it against nuclease degradation.

Circular dichroism (CD) spectroscopy provides an insight into the conformational changes that take place in the structure of the double stranded DNA. Cationic surfactants bind to the native B-form of DNA and convert it into the ψ-form, which has a less number of base pairs (9.33/turn) in comparison to the original 10 base pairs/turn.[52] The native B-form of DNA shows a positive band at 277 nm and a negative band at 245 nm in the CD spectrum in HEPES buffer. A shift of the positive peak to higher values with complete flattening, and an increased intensity of the negative band are indicative of condensation of DNA from the native B-phase to the ψ-phase.[53] Combining pDNA with GA liposomal formulation causes a change in the original B-form of the pDNA to ψ-form. GAs were observed to be effective in converting the B-form of DNA to the ψ−form as seen by comparing the results obtained in these experiments (Figure S2). Molecular structures of the GAs and the nature of DNA both are responsible for effective compaction of the DNA. Using equivalent amounts of GAs under the same experimental conditions, monohydroxyethylated GAs (B-type) showed more effective condensation of the pDNA compared to the remaining dimethylated (A-type) or di(hydroxyethyl)ated (C-type) GAs.

2.6. Transfection Studies Using the β-Gal Reporter Plasmid. *2.6.1. Transfection Studies in the Absence of Serum [Fetal Bovine Serum].* The transfection efficacy of each GA either alone or with DOPE as a helper lipid in the lipoplexes was evaluated in two cell lines (A549 and HeLa, cultured in DMEM) at N/P ratios of 0.5, 1, 2, 3, 4, and 6 using β-Gal reporter plasmid. The transfection efficacy of the GA formulations (either GA alone or GA along with the helper lipid) is directly indicated by the quantum of β-galactosidase protein expressed in the cells. The results (Figures S3 to S18) so obtained showed that all the formulations composed of GAs along with the helper lipid DOPE exhibited higher β-Gal expression than the formulations containing the GAs all alone. This could be because of early release of the lipoplex containing the DNA cargo at the endosomal stage inside the cells.[54] A N/P ratio of 0.5 was not found to be effective in transfection of the genetic material and a high N/P ratio of 6 also did not offer any advantage over the lower ratios. GAs

https://doi.org/10.1021/acsomega.1c03667
ACS Omega 2021, 6, 33370−33388

Table 3. Highest Transfection Efficacies of the GA Formulations [GA with DOPE in Optimum Ratios of 1:1 (a), 1:2 (b), or 1:3 (c)] in the Absence of Serum

series-III			series-IV		
GA formulation (optimum N/P ratio)	β-galactosidase activity (mean ± S.D.) (mU)		GA formulation (optimum N/P ratio)	β-galactosidase activity (mean ± S.D.) (mU)	
	A549 cell line	HeLa cell line		A549 cell line	HeLa cell line
9AIa (4)	1.18 ± 0.05	1.55 ± 0.13	**10AIa** (3)	1.70 ± 0.12	1.88 ± 0.11
9BIb (1)	1.11 ± 0.20	2.03 ± 0.46	**10BIa** (2)	1.90 ± 0.26	3.21 ± 0.53
9BIIa (2)	0.62 ± 0.14	0.74 ± 0.12	**10BIIb** (2)	0.95 ± 0.21	1.23 ± 0.25
9BIIIa (2)	1.06 ± 0.20	1.97 ± 0.38	**10BIIIa**	2.12±0.31 (3*)	3.58±0.28 (2*)
9BIVa (3)	1.02 ± 0.17	1.12 ± 0.14	**10BIVa** (2)	1.05 ± 0.09	1.22 ± 0.19
9CIa (2)	1.15 ± 0.25	1.72 ± 0.16	**10CIIIb** (1)	2.06 ± 0.10	2.19 ± 0.29
9CIIb (3)	0.94 ± 0.23	1.04 ± 0.13	**10CIVa** (4)	0.99 ± 0.16	1.12 ± 0.14
9CIIIa (1)	1.33 ± 0.24	1.63 ± 0.31	**DOTAP−DOPE**	1.37 ± 0.12	1.94 ± 0.38
9CIVa (3)	0.85 ± 0.13	1.10 ± 0.13	**DCC−DOPE**	1.68 ± 0.24	2.47 ± 0.31
*optimum N/P ratio			**lipofectamine**	2.07 ± 0.35	3.12 ± 0.35

(**9BI**, **9CIII**, and **10CIII**) offered optimum results at a N/P ratio of 1:1, GAs (**9BII**, **9BIII**, **9CI**, **10BI**, **10BII**, and **10BIV**) yielded optimum efficacy at a N/P ratio of 2, GAs (**9BIV**, **9CII**, **9CIV**, and **10AI**) gave optimum efficacy at a N/P ratio of 3, while GAs (**9AI** and **10CIV**) gave optimum results at a N/P ratio of 4 in both the cell lines. GA (**10BIII**) was an exception in which a N/P ratio of 3 was found to offer the best results in A549 and a N/P ratio of 2 yielded the best results in HeLa cell lines. The order of transfection efficacy of the GA formulations alone, and GA formulations containing the helper lipid DOPE in the ratios [1:1 (**a**), 1:2 (**b**) or 1:3 (**c**)] at their optimum N/P ratios was found to be **10BIIIa** > **10CIIIb** > **10BIa** > **10AIa** > **9CIIIa** > **9AIa** > **9CIa** > **9BIb** > **9BIIIa** > **10BIVa** > **9BIVa** > **10CIVa** > **10BIIb** > **9CIIb** > **9CIVa** > **9BIIa** in A549, and **10BIIIa** > **10BIa** > **10CIIIb** > **9BIb** > **9BIIIa** > **10AIa** > **9CIa** > **9CIIIa** > **9AIa** > **10BIIb** > **10BIVa** > **10CIVa**∼**9BIVa** > **9CIVa** > **9CIIb** > **9BIIa** in HeLa cancer cell lines (Table 3).

In our earlier study,[44] it was observed that the tetramethylene hydrocarbon chain as the spacer offered a higher transfection efficacy than the hexamethylene chain. In the current study, it was found out that the polar linker diethyleneoxy (**10BIIIa** and **10CIIIb**) offered better results than the more rigid *p*-xylenyl linker (**9BIb**, **9CIa**, or **9CIIIa**) in both the series in both of the cancer cell lines. It may be noted that diethyleneoxy is not only more polar than the simple hydrocarbon chain (whether CH_4 or CH_6) but it also has an intermediate length between CH_4 and CH_6. That means, the chain length equivalent to C_5 with a higher polarity than the hydrocarbons is responsible for offering a higher transfection efficacy than the rest of the linkers. The best transfection efficacy was shown by the GA formulation (**10BIIIa**), which was even better than that shown by the standard formulations (**Lipofectamine**, **DCC−DOPE**, or **DOTAP−DOPE**), and also by the earlier reported[44] best GA (**5d**) having the same structural features as **10BIII** except for the spacer. Among the head groups, mixed-type results were obtained for monohydroxyethyl and di(hydroxyethyl) head groups, both of which offered a higher transfection efficacy than the dimethyl head group. GAs with monohydroxyethyl groups offered slightly better results than the GAs having di(hydroxyethyl) head groups. These observations were in tune with our earlier observations.[44] Tetradecyl (**9CIIIa**, **10BIIIa**, and **10CIIIb**) and hexadecyl (**9AIa**, **9BIb**, **9CIa**, and **10AIa**) lipophilic chains offered better transfection than the remaining two lipophilic chains (i.e., dodecyl and octadecyl). The impact of tetradecyl and hexadecyl lipophilic chains on transfection efficacy was observed to be higher than that of dodecyl and octadecyl chains in our report[44] also. Overall, much higher transfection was observed in HeLa cell lines than in A549 cell lines for all the reported GAs. A higher transfection susceptibility of HeLa cells than A549 cells could be the reason for this observation.

Moreover, a decrease in the N/P ratio from 4 to 1 or 2 to achieve the highest transfection efficacy indicated that a smaller molar concentration of hydroxyethylated GAs is needed to exhibit the best transfection results compared to the non-hydroxyethylated GAs. Figures 5 and 6 show the compiled

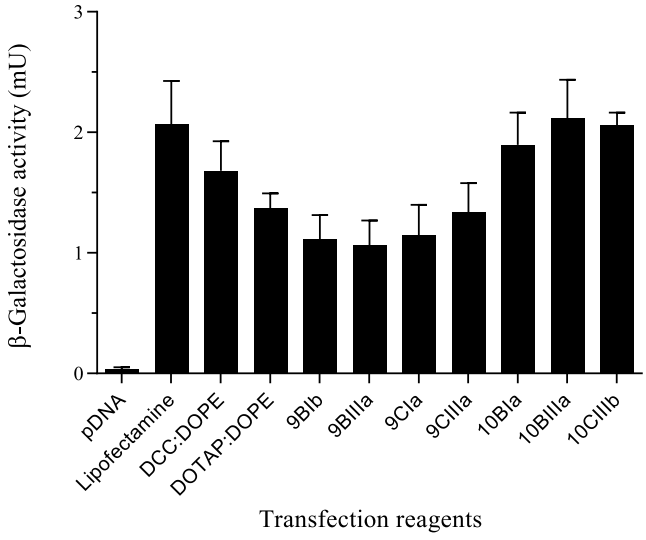

Figure 5. Comparative transfection efficacies of the best GA formulations in the A549 cell line at their optimized N/P ratios.

results of GA formulations exhibiting good *β*-Gal expression in both the cell lines vis-à-vis the expression shown by the naked pDNA and the commercially available transfection reagents (i.e., DOTAP−DOPE, DCC−DOPE, or Lipofectamine liposomes). It can be seen that the naked pDNA without inclusion of any vector exhibited a very low level of expression of 0.077 and 0.04 mU in HeLa and A549 cell lines, respectively.

2.6.2. Effect of Serum on the Transfection Efficacy of GAs. It is known that serum decreases the transfection efficacies of

https://doi.org/10.1021/acsomega.1c03667
ACS Omega 2021, 6, 33370−33388

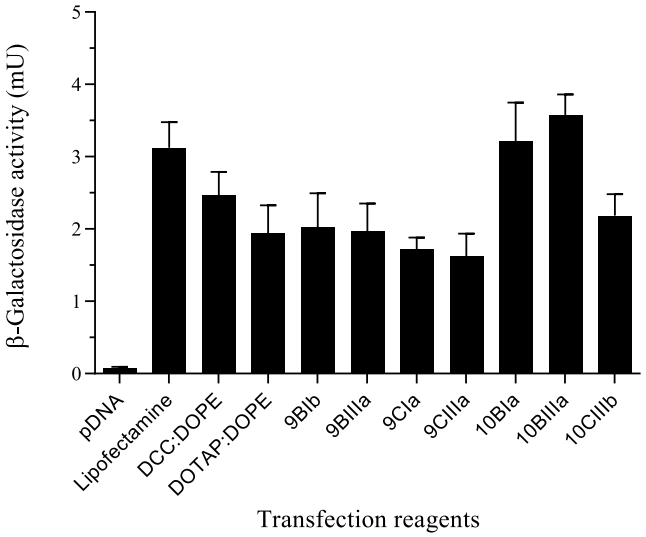

Figure 6. Comparative transfection efficacies of the best GA formulations in the HeLa cell line at their optimized N/P ratios.

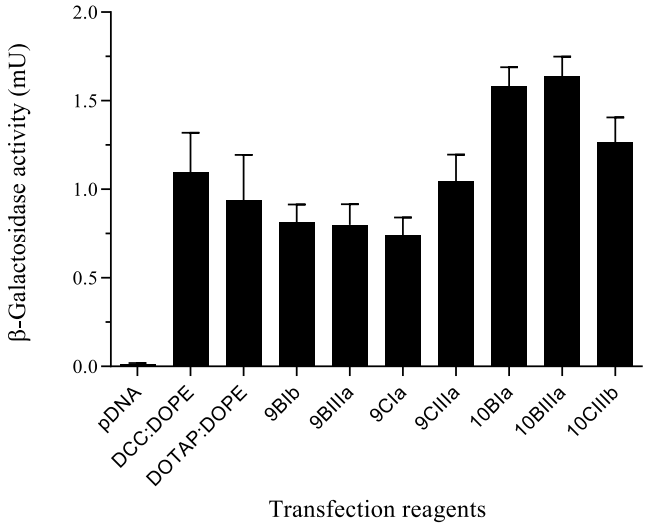

Figure 7. Comparative transfection efficacies of the best GA formulations in the A549 cell line in the presence of 10% FBS.

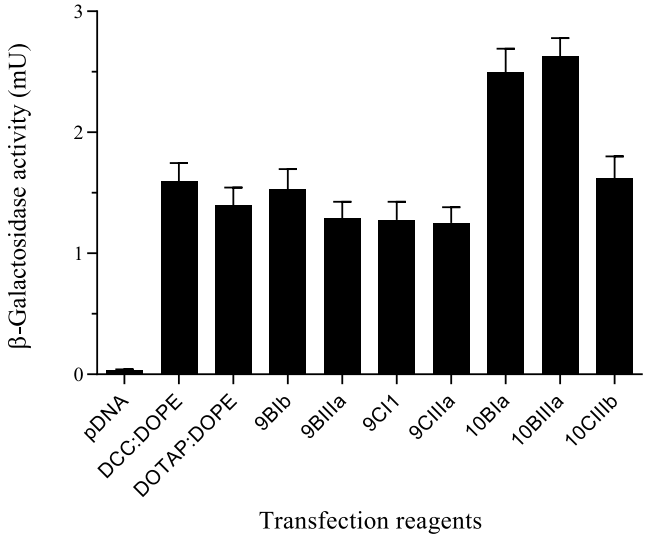

Figure 8. Comparative transfection efficacies of the best GA formulations in the HeLa cell line in the presence of 10% FBS.

the gene delivery vectors. Therefore, it was decided to check the impact of serum [additional 10% fetal bovine serum (FBS) in DMEM] on the transfection efficacies of the GA formulations offering the best results in DMEM in both the cell lines. A common decline in transfection efficacies was observed in both the cell lines for all the chosen formulations (Table 4). The standard formulations (DCC−DOPE and DOTAP−DOPE) used in the study also exhibited a declining trend in their transfection efficacy in the presence of serum. The GA formulation (**10BIIIa**) offered the highest transfection efficacy in the presence of serum also. The order of transfection efficacy was more or less maintained as was observed in the absence of serum. The order of transfection efficacy in the A549 cell line was **10BIIIa** > **10BIa** > **10CIIIb** > **9CIIIa** > **9BIb** > **9BIIIa** > **9CIa** (Figure 7), while in the HeLa cell line the order was **10BIIIa** > **10BIa** > **10CIIIb** > **9BIb** > **9BIIIa** > **9CIa** > **9CIIIa** (Figure 8).

2.6.3. Transfection Efficacies of GAs in the Presence of Cholesterol. Cholesterol is reported to confer serum compatibility to the vectors used for delivery of genes.[55] Keeping this report in mind, it was planned to incorporate cholesterol in the lipoplex formulations of the synthesized GAs and evaluate their transfection efficacies in the absence and in the presence of serum (10% FBS). Cholesterol was incorporated into the formulations in two different ratios [GA/DOPE/cholesterol in the ratio of 1:1:1 Formulation (d), and 1:1:0.5 Formulation (e)].

In the A459 cell line, **10BId** and **10BIIId** showed the highest β-Gal expression of 2.06 and 2.43 mU, respectively, at

Table 4. Comparative Transfection Efficacies of GA Formulations in the Absence and Presence of Serum

	β-galactosidase activity (mean ± S.D.) (mU)			
	in the absence of serum		in the presence of serum	
GA formulation	A549 cell line	HeLa cell line	A549 cell line	HeLa cell line
9Bib	1.11 ± 0.20	2.03 ± 0.46	0.78 ± 0.10	1.48 ± 0.16
9BIIIa	1.06 ± 0.20	1.97 ± 0.38	0.77 ± 0.11	1.27 ± 0.13
9CIa	1.15 ± 0.25	1.72 ± 0.16	0.73 ± 0.10	1.24 ± 0.15
9CIIIa	1.33 ± 0.24	1.63 ± 0.31	1.03 ± 0.14	1.23 ± 0.13
10BIa	1.90 ± 0.26	3.21 ± 0.53	1.57 ± 0.10	2.48 ± 0.19
10BIIIa	2.12±0.31	3.58±0.28	1.62±0.11	2.62±0.15
10CIIIb	2.06 ± 0.10	2.19 ± 0.29	1.25 ± 0.14	1.56 ± 0.18
DOTAP−DOPE	1.37 ± 0.12	1.94 ± 0.38	0.92 ± 0.25	1.38 ± 0.15
DCC−DOPE	1.68 ± 0.24	2.47 ± 0.31	1.11 ± 0.22	1.58 ± 0.15

https://doi.org/10.1021/acsomega.1c03667
ACS Omega 2021, 6, 33370−33388

Table 5. Effect of Cholesterol on the Transfection Efficacy of the Selected GA Formulations

		transfection efficacy (mean ± S.D.) (mU)			
		in the absence of serum		in the presence of serum	
GA	formulation	A549	HeLa	A549	HeLa
10BI	without cholesterol				
	10BIa [GA + DOPE (1:1) + pDNA]	1.90 ± 0.26	3.21 ± 0.53	1.57 ± 0.10	2.48 ± 0.19
	with cholesterol (Chol)				
	10BId [GA + DOPE + Chol (1:1:1) + pDNA]	**2.06±0.23**	**3.29±0.31**	**1.57±0.28**	**2.93±0.25**
	10BIe [GA + DOPE + Chol (1:1:0.5) + pDNA]	1.90 ± 0.24	3.38 ± 0.31	1.47 ± 0.25	2.81 ± 0.26
10BIII	without cholesterol				
	10BIIIa [GA + DOPE (1:1) + pDNA]	2.12 ± 0.31	3.58 ± 0.28	1.62 ± 0.11	2.62 ± 0.15
	with cholesterol (Chol)				
	10BIIId [GA + DOPE + Chol (1:1:1) + pDNA]	**2.43±0.32**	**3.61±0.28**	**2.14±0.23**	**3.09±0.27**
	10BIIIe [GA + DOPE + Chol (1:1:0.5) + pDNA]	2.20 ± 0.32	3.70 ± 0.24	2.04 ± 0.31	2.77 ± 0.23

N/P ratios of 2 and 3 in the absence of serum (Table 5, and Figures 9 and 10). However, in the presence of 10% serum,

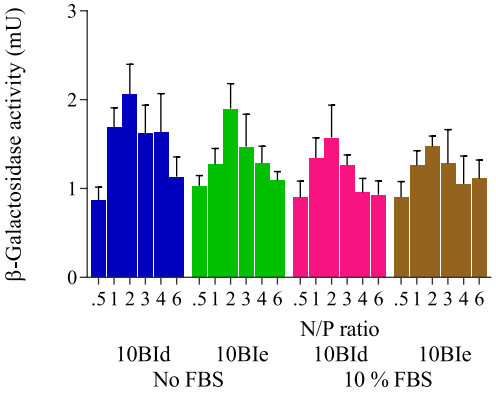

(A)

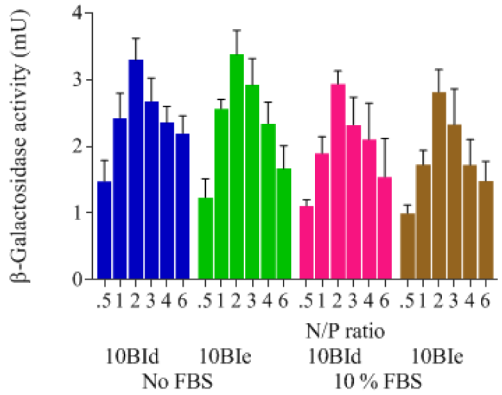

(B)

Figure 9. Transfection efficacies of **10Bid** (**10BI**/DOPE/cholesterol; 1:1:1) and **10BIe**(**10BI**/DOPE/cholesterol; 1:1:0.5) in (A) A549 and (B) HeLa cell lines in the absence and the presence of serum (10% FFBS).

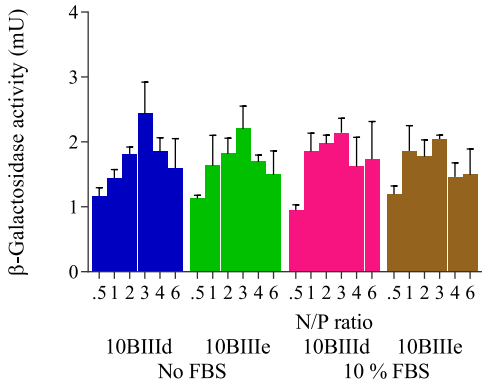

(A)

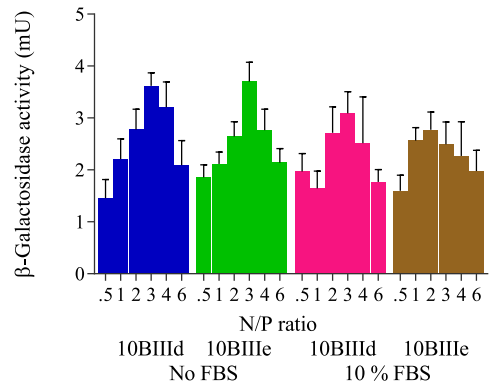

(B)

Figure 10. Transfection efficacies of **10BIIId** (**10BIII**/DOPE/cholesterol; 1:1:1) and **10BIIIe** (**10BIII**/DOPE/cholesterol; 1:1:0.5) in (A) A549 and (B) HeLa cell lines in the absence and presence of serum (10% FBS).

these formulations showed 1.57 and 2.14 mU β-Gal expression at these N/P ratios. In the HeLa cell line, **10BIe** and **10BIIIe** showed the highest β-Gal expression of 3.38 and 3.70 mU, respectively, at N/P ratios of 2 and 3 in the absence of serum, while these formulations exhibited the expressions of 2.81 and 2.77 mU, respectively, of β-Gal in the presence of 10% serum at a N/P ratio of 2.

2.7. Fluorescence-Assisted Cell Sorting Studies.

Determining β-galactosidase activity as a measure of transfection efficacy of the synthesized GAs is a good indicator of the effectiveness of the DNA-carrying capacity of a delivery system, but to know the number of transfected cells by the vector is also an important criterion to assess its efficiency. This aim was fulfilled by performing fluorescence-assisted cell sorting (FACS) studies. GA formulations showing promising results in β-Gal expression were chosen for FACS studies,

https://doi.org/10.1021/acsomega.1c03667
ACS Omega 2021, 6, 33370−33388

using the expression of green fluorescence plasmid (GFP) by the transfected cells in a 24-well format. The fluorescence of GFP was observed and captured under a fluorescence microscope. The fluorescence images of GFP plasmid for the formulations (**10BIa**, **10BId**, **10BIIIa**, and **10BIIId**) are shown in Figures 11 and 12 in A549 and HeLa cells,

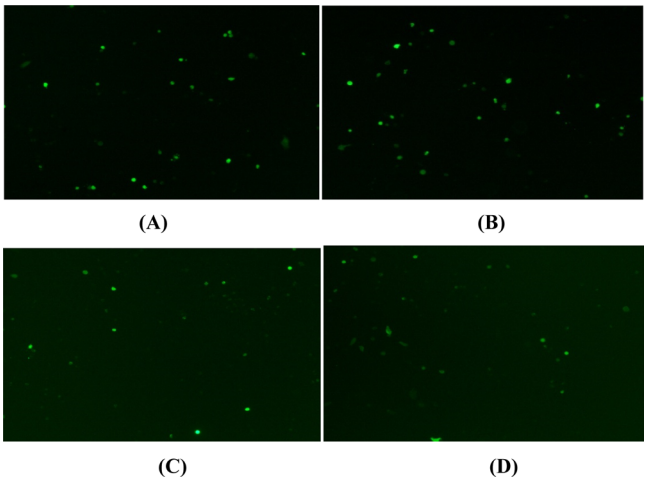

Figure 11. Fluorescence images of GFP expression in A549 cells in the absence of serum: (A) **10BIIIa**, (B) **10BIIId**, (C) **10BIa**, and (D) **10BId** at their optimum N/P ratios.

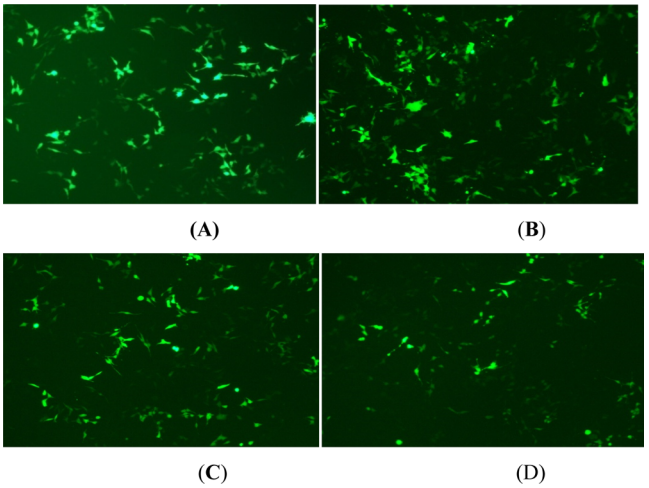

Figure 12. Fluorescence images of GFP expression in HeLa cells in the absence of serum: (A) **10BIIIa**, (B) **10BIIId**, (C) **10BIa**, and (D) **10BId** at their optimum N/P ratios.

respectively, in the absence of serum. Figures 13 and 14 show the percent of cells transfected with GFP plasmid using these formulations in comparison to the plain GFP plasmid (negative control) and standard formulations (DOTAP/DOPE, DCC/DOPE, or Lipofectamine 2000 liposomes) in A549 and HeLa cells, respectively, in the absence of serum. It was found out that formulations containing cholesterol along with the helper lipid DOPE (**10BId** and **10BIIId**) caused a higher number of transfected cells in comparison to the formulations without cholesterol (**10BIa** and **10BIIIa**). This was a common observation for both the cell lines A549 and HeLa in the absence of serum. The order of efficacy for the formulations in the absence of serum was **10BIIId** > **10bId** > **10BIIIa** > **10BIa** in the A549 cell line and **10BIIId** > **10BIIIa**

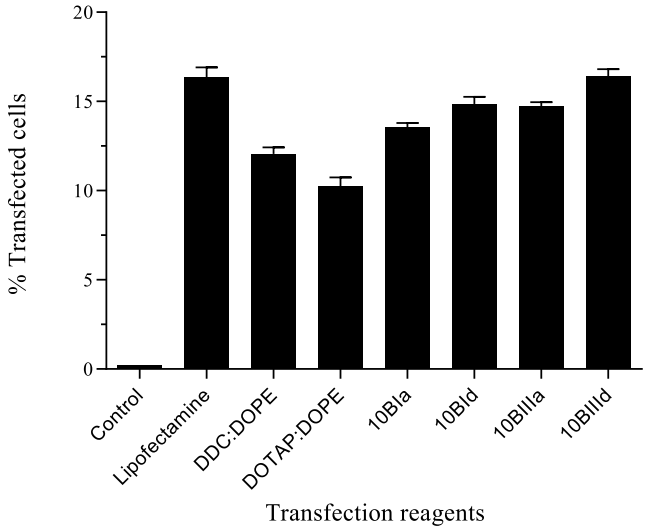

Figure 13. FACS studies of optimized formulations (at optimum N/P ratios) using GFP plasmid in A549 cells in the absence of serum.

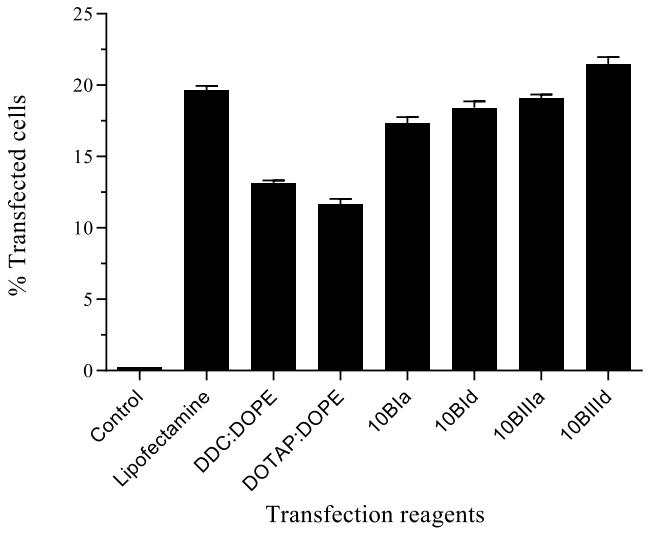

Figure 14. FACS studies of optimized formulations (at optimum N/P ratios) using GFP plasmid in HeLa cells in the absence of serum.

> **10BId** > **10BIa** in the HeLa cell line. In the absence of serum formulation, (**10BIIId**) offered even better results than the standard Lipofectamine formulation in both the cell lines (Table 6).

The percentage of transfected cells by the optimized GA formulations at their optimized N/P ratios in A549 and HeLa cells, respectively, in the presence of serum is shown in Figures 15 and 16. Both of the cholesterol-containing formulations (**10BId** and **10BIIId**) showed a significant increase in the percentage of transfected cells in comparison to the DOTAP/DOPE or DCC/DOPE liposomal formulations in both of the cell lines. Cholesterol-containing GA formulations (**10BId** and **10BIIId**) yielded a higher percentage of transfected cells in comparison to the cholesterol-deficient formulations (**10BIa** and **10BIIIa**) in the presence of serum in both of the cell lines. The order of efficacy in the presence of serum was found to be **10BIIId** > **10BId** > **10BIIIa** > **10BIa** in both the cell lines. These results indicated that incorporation of cholesterol improved serum compatibility of the lipoplexes.

https://doi.org/10.1021/acsomega.1c03667
ACS Omega 2021, 6, 33370−33388

Table 6. Transfection Efficacy of the Selected Formulations Using FACS

	transfection efficacy (% transfected cells) (mean ± S.D.)			
	in absence of serum		in presence of serum	
Formulation	A549	HeLa	A549	HeLa
10BIa	13.1 ± 0.25	16.5 ± 0.43	7.3 ± 0.43	9.8 ± 0.36
10Bid	14.43 ± 0.41	17.95 ± 0.10	9.1 ± 0.35	12.6 ± 0.39
10BIIIa	14.41 ± 0.25	18.78 ± 0.13	8.49 ± 0.31	10.71 ± 0.37
10BIIId	16.18±0.44	21.0±0.49	11.13±0.39	15.57±0.33
DCC−DOPE	11.5 ± 0.35	12.8 ± 0.17	7.8 ± 0.13	9.7 ± 0.38
DOTAP−DOPE	9.8 ± 0.51	11.0 ± 0.37	7.4 ± 0.24	7.8 ± 0.41
Lipofectamine	15.94 ± 0.55	19.32 ± 0.29	ND	ND

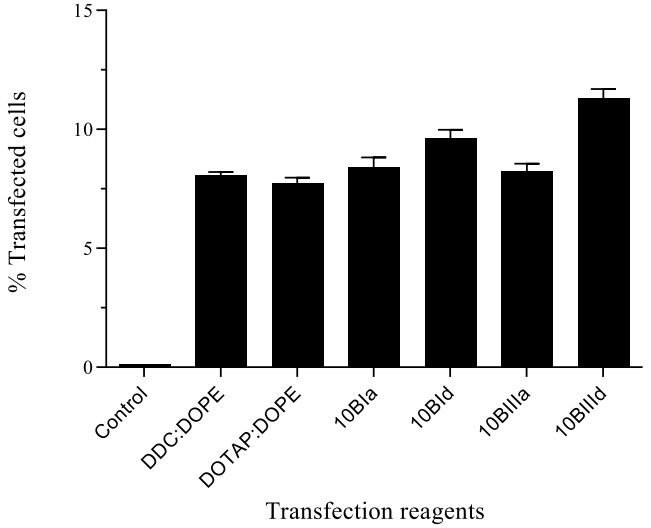

Figure 15. FACS studies of the optimized formulations (at optimum N/P ratios) using GFP plasmid in A549 cells in the presence of serum.

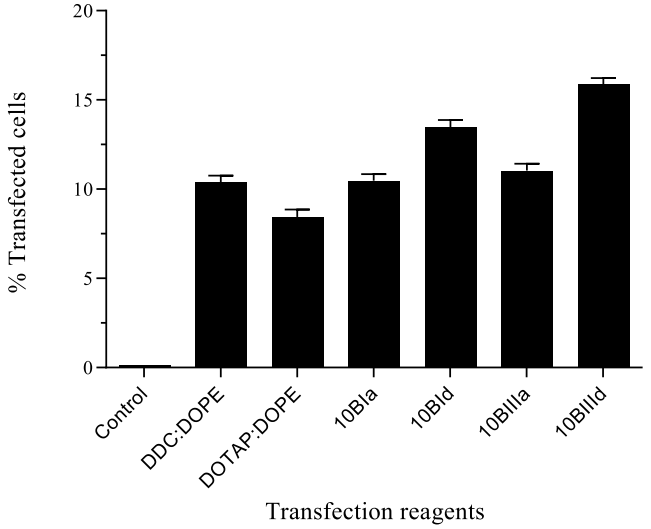

Figure 16. FACS studies of optimized formulations (at optimum N/P ratios) using GFP plasmid in HeLa cells in the presence of serum.

2.8. Intracellular Trafficking of the Lipoplexes Using Confocal Microscopy. The GA formulation (**10BIIId**), which offered the best results in the in vitro transfection and FACS studies was chosen for the study of intracellular trafficking of the lipoplexes using confocal microscopy. The nuclear staining dye 4′,6′-diamidino-2-phenylindole (DAPI) was used to tag the lipoplexes by incubating them with the dye overnight. Cells of both the cell lines (A549 and HeLA) were incubated with the dye-tagged lipoplexes in a 6-well format, and they were harvested at 10, 20, and 30 min after incubation and fixed. Representative images of the incubated HeLa cell lines are shown in Figure 17. The first row of Figure 17 shows the control group of cells without any lipoplex treatment. The phase contrast images of the cells are shown in the first two images of each row. The third image is a merged one showing the blue-stained nucleus and morphology of the cells. The second row (Figure 17) shows lipoplexes (green-colored dots) entering in the cytoplasm of the cells after 10 min of incubation. The third row (Figure 17) shows the accumulation of the lipoplexes (green-colored dots) inside the nuclei of the cells after 20 min of incubation. The fourth row (Figure 17) shows further accumulation of the lipoplexes (green-colored dots) inside the nuclei of the cells after 30 min of incubation.

2.9. Cytotoxicity Studies of GA Formulations by the MTT Assay. A good gene delivery vector should possess not only a high degree of transfection efficacy but should also be non-toxic to the cells at the same time. Cytotoxicity is an important parameter for selecting a suitable delivery carrier for the nucleic acid cargo in gene delivery. Formulations containing GAs (**9AI**, **9BI**, **9BIII**, **9CI**, **9CIII**, **10AI**, **10BI**, **10BIII**, and **10CIII**), which exhibited good transfection efficacy of the reporter gene (pDNA), were evaluated for cell toxicity/viability using the MTT assay under conditions identical to those maintained in their transfection studies using different N/P ratios. The results are shown in Figures S19 to S27.

The viability of untreated cells was taken as 100%. All of the GA formulations evaluated by the MTT assay showed N/P ratio-dependent cell viability. An increase in the N/P ratio in the lipoplex formulations from 0.5 to 6 led to an increase in their toxicity because formulations having higher N/P ratios had higher net quantities of the positively charged GAs. A comparison was made by evaluating the standard formulations of DOTAP−DOPE and DCC−DOPE also in both the cell lines (Figures 18 and 19). It can be seen that cell viabilities for the selected GA formulations were more or less matching the viabilities of the standard formulations at their optimum N/P ratios. DOTAP−DOPE and DCC−DOPE standard formulations exhibited 83.38 and 89.2%, and 82.6 and 87.2% cell viabilities in A549 and HeLa cell lines, respectively. No significant difference in the toxicity of GA formulations could be seen except for formulation (**9CIa**), which proved to be a bit more toxic than the rest, for both the cell lines in the MTT assay.

https://doi.org/10.1021/acsomega.1c03667
ACS Omega 2021, 6, 33370−33388

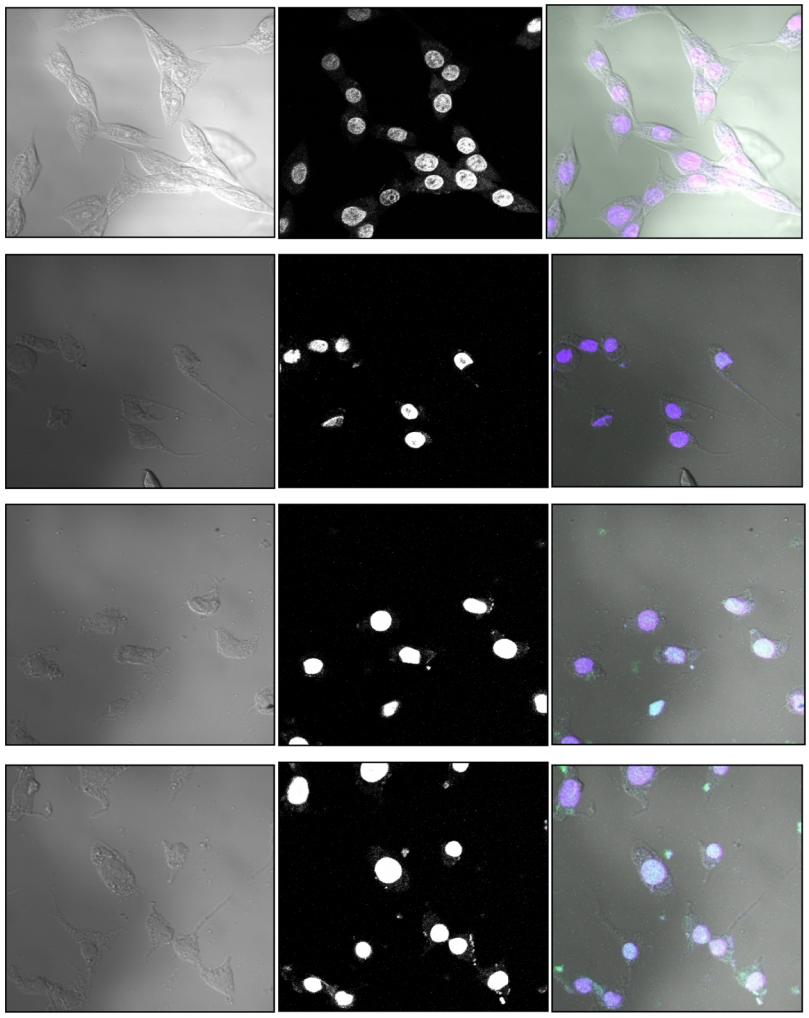

Figure 17. Confocal images of pDNA uptake in HeLa cells. First row, the control group; second row, after 10 min incubation; third row, after 20 min incubation; and fourth row, after 30 min of incubation period.

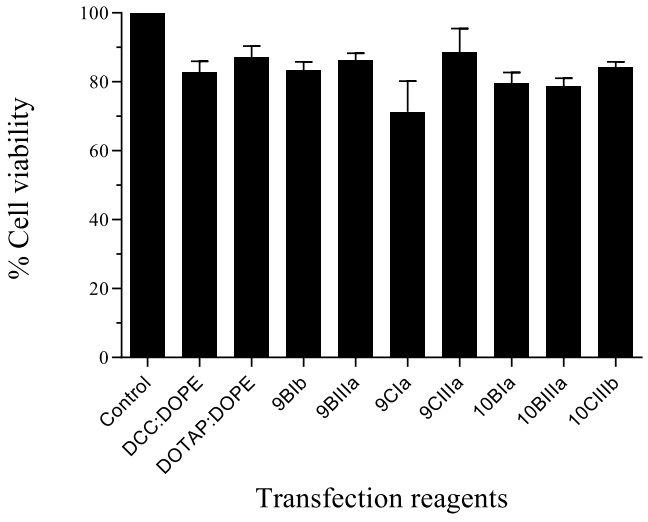

Figure 18. Percent cell viabilities of the major GA formulations and the standard formulations at their optimum N/P ratios in A549 cell lines.

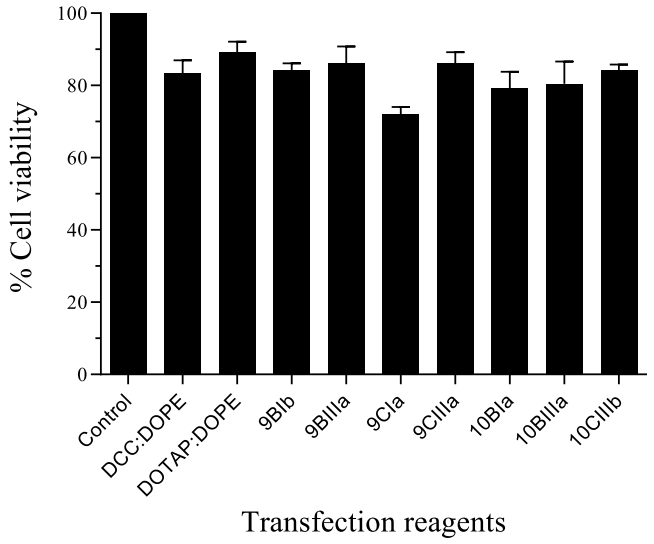

Figure 19. Percent cell viabilities of the major GA formulations and the standard formulations at their optimum N/P ratios in HeLa cell lines.

2.10. Biodistribution Studies. After subjecting the GA formulations to different tests to check their transfection efficacy and cellular toxicity, it became clear that one (**10BIII**) of the synthesized GAs has the potential to be used as an efficient delivery carrier for nucleic acid cargos when

https://doi.org/10.1021/acsomega.1c03667
ACS Omega 2021, 6, 33370−33388

formulated in combination with helper lipids such as DOPE and cholesterol. Another important criterion for gene delivery is to know the fate of the lipoplexes, that is, how are the lipoplexes getting distributed in the body when administered by parenteral route? To get an answer for this question, it was planned to study the biodistribution of the lipoplex formulation of the chosen GA (i.e., **10BIIId**). For this purpose, the lipoplexes were tagged with technetium-99m (^{99m}Tc). The purpose of radiolabeling of the lipoplexes was to assess their distribution pattern in various organs in the animal model after their intravenous administration. ^{99m}Tc has been the most commonly used radionuclide to radiolabel various drug delivery carriers because of its wide availability, low cost, favorable imaging properties, and a half-life of 6 h.[56] The biodistribution study was performed by administrating the ^{99m}Tc-labeled lipoplexes through the tail vein. The complexes of lipoplexes and ^{99m}Tc were prepared by a direct radiolabeling technique as discussed in the Experimental Section. The radiolabeled lipoplex formulation equivalent to 15 μg of pDNA was injected into the tail vein of rats and the organs were harvested at fixed time intervals of 1, 6, and 24 h. Percent radioactivity was determined in the harvested organs at the given time intervals as shown in Figure 20. In the first 1 h, the

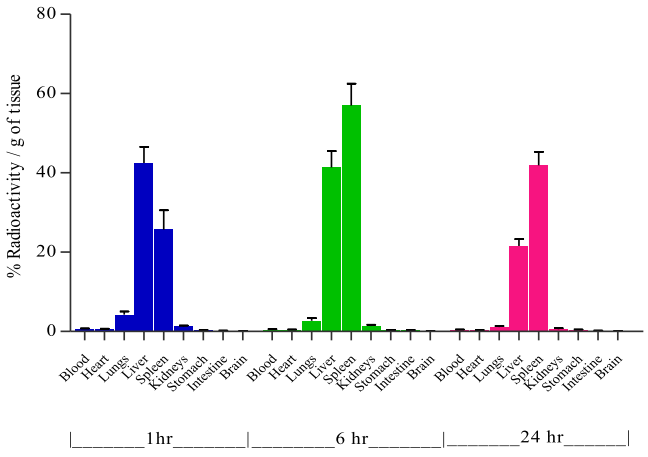

Figure 20. Accumulation of ^{99m}Tc-labeled lipoplexes (**10BIIId**) in various organs of rat at various time intervals.

lipoplexes accumulated in the liver, spleen, lungs, and kidneys in that order, but at 6 h and later, a higher amount of radioactivity was observed in the spleen than in the liver. Of course, radioactivity decreased at 24 h in almost all organs, but it was still very high in two vital organs, that is, the spleen and the liver.

3. CONCLUSIONS

Two main series of GAs differing in the chemical nature of the linkers have been synthesized. One series has a *p*-xylyl linker (Series-III, compounds bearing number **9**), while the other one has a more hydrophilic 3-oxypentyl chain (Series-IV, compounds bearing number **10**) joining the two cationic heads. The head group polarity was changed from dimethyl (subseries-A) to hydroxyethylmethyl (subseries-B) and di-(hydroxyethyl) (subseries-C). In both series of compounds, the lipophilic chain was varied from hexadecyl (**I**) to dodecyl (**II**), tetradecyl (**III**), and octadecyl (**III**) moieties. All the GAs offered very low cmc values suggesting very good surface-active properties of the synthesized GAs. The GAs were used in different N/P ratios with pDNA in the lipoplex formulations. The agarose gel retardation assay and CD studies of the lipoplexes indicated tight binding of the GAs with pDNA, and the GAs caused condensation of the pDNA making it a compact structure, ideal for penetration into the target cells. DNase I digestion studies indicated that all the GAs at 1 or higher N/P ratios protected the pDNA from the enzyme degradation. All the GAs either all alone or along with helper lipid DOPE, in the form of lipoplexes, were evaluated for their potential application as vectors for delivery of pDNA for transfecting A549 and HeLa cell lines using β-galactosidase plasmid as the nucleic acid load. In the transfection studies, GAs of Series-IV (compounds no. **10**) having the diethyleneoxy linker, the monohydroxyethyl head group (subseries-**B**), and the hexadecyl or tetradecyl lipophilic moieties offered the best results. The highest transfection efficiency was shown by the GA formulation (**10BIIIa**), which was even higher than that of the standard Lipofectamine formulation. The presence of serum in the medium decreased the transfection efficiency of the GA formulations but inclusion of cholesterol in the formulations (Formulations d and e) improved the transfection efficacy even in the presence of serum. Use of GFP in the FACS studies also indicated a higher number of transfected cells by the GA (**10BIII**) in the form of formulation (**10BIIId**) containing cholesterol than the standard Lipofectamine formulation. Confocal microscopy also showed accumulation of the lipoplexes of **10BIII** in the cytoplasm of A549 and HeLa cells. A higher level of transfection tendency was observed in HeLa cells than in A549 cells in studies with all of the GAs. All the synthesized GAs showed dose-dependent toxicity in the MTT assay. The survival percentage varied from 80 to 90% for the GAs at their optimum N/P ratios in the lipoplexes. Biodistribution studies in rats using the ^{99m}Tc-labeled lipoplex (**10BIIId**) indicated that the lipoplexes were preferentially taken up by organs such as the liver, spleen, lungs, and kidneys. Overall, the GA (**10BIII**) offered much better results than the GAs from Series-I and Series-II earlier reported by us, and even better results than the standard transfection agents such as DOPE−DOTAP, DCC−DOTAP, or Lipofectamine. The newly reported GA (**10BIII**) exhibiting the best results among the compounds from the current Series-III and -IV and from our earlier reported compounds of two series (Series-I and -II) has the potential to be deployed as a synthetic carrier for transfecting cells with the desired nucleic acid load for gene therapy to combat various genetic disorders.

4. EXPERIMENTAL SECTION

4.1. Materials. Amines such as diethanolamine, *N*-methylethanolamine, *N*-hexadecyl-*N*,*N*-dimethylamine, and reagents such as dibromobutane, *o*-nitrophenol-β-galactopyranoside (ONPG), Dulbecco's modified Eagle's medium (DMEM), diethylenetriaminepentaacetic acid, stannous chloride dihydrate ($SnCl_2 \cdot H_2O$), DAPI, and enzyme-like β-galactosidase (140 U/mg) were procured from Sigma-Aldrich. Trypsin−EDTA, FBS, phosphate buffered saline (PBS), antibiotic cocktail (penicillin−streptomycin−amphotericin-B), 3-(4,5-dimethylthiazol-2yl)-2,5-diphenyltetrazolium bromide (MTT), and Nonidet P-40 (NP-40) were purchased from Hi-Media, Mumbai. Molybdenum-99 as the precursor of ^{99m}Tc was obtained from Center for Radiopharmaceutical Division (Northern Region), Board of Radiation and Isotope Technology (BRIT, Delhi, India). ^{99m}Tc as sodium pertechnetate was separated from molybdenum-99 using the solvent

https://doi.org/10.1021/acsomega.1c03667
ACS Omega 2021, 6, 33370−33388

extraction method. Silica gel instant thin-layer chromatography (TLC) plates (ITLC-SG) were purchased from Gelman Science Inc.

A549 and HeLa cell lines were obtained from the National Centre for Cell Sciences (NCCS), Pune, India, and the cells were cultured in DMEM along with FBS (10%) containing the antibiotic cocktail penicillin−streptomycin−amphotericin-B (1%) in a CO_2 incubator at 37 °C.

pDNAs of β-galactosidase (i.e., CMV.SPORT-βgal), and of GFP were gifted by IICT, Hyderabad, India. pDNAs for both the proteins were transformed into *E. coli* DH5α using the Transform Aid bacterial transformation kit and purified and isolated with the Qiagen plasmid purification kit. The A_{260}/A_{280} ratio (determined by UV absorption spectrophotometer) and gel electrophoresis were used for ascertaining the purity of pDNA.

4.2. Chemical Synthesis. The purity of the solvents and reagents was checked before use and purified using conventional methods wherever required. Progress and completion of the reactions, and purity of the reaction products were checked by TLC using silica gel GF (Merck) and suitable solvents as the mobile phase, and visualizing under UV light or by exposure to iodine vapors. Melting points were measured on a silicone oil bath-type melting point apparatus, Veegomake, Mumbai, and were uncorrected. IR spectra were recorded on a Bruker FT-IR spectrometer, model alpha, using the KBr disc method or on ATR in the case of liquid samples. $CDCl_3$ or DMSO-d_6 was used as the solvent for obtaining the PMR spectra on a Bruker 300 MHz spectrometer. Peaks are reported in δ ppm in comparison to TMS. Elemental analyses were performed using a Thermo Fisher FLASH 2000 elemental analyzer. All of the GAs offered the results within ±0.4% of the theoretically calculated values of carbon, hydrogen, and nitrogen elements.

4.3. Synthesis and Characterization of GAs. *4.3.1. Preparation of Tertiary Amines.* The tertiary amines *N*-hexadecyl-*N*-methylethanolamine (**5I**), *N*-dodecyl-*N*-methylethanolamine (**5II**), *N*-methyl-*N*-tetradecylethanolamine (**5III**), *N*-methyl-*N*-octadecylethanolamine (**5IV**), *N*,*N*-di(2-hydroxyethyl)-*N*-hexadecylamine (**6I**), *N*-dodecyl-*N*,*N*-di(2-hydroxyethyl)amine (**6II**), and *N*,*N*-di(2-hydroxyethyl)-*N*-tetradecylamine (**6III**) were prepared as reported earlier.[44]

4.3.1.1. Method-A. *N*,*N*-Di(2-hydroxyethyl)-*N*-octadecylamine (**6IV**): the title compound was prepared from diethanolamine (**3**) (4.23 mL, 44 mmol), 1-bromooctadecane (**4IV**) (13.65 mL, 40 mmol), and anhydrous sodium carbonate (2.32 g, 22 mmol) in dry ethanol. The reaction mixture was refluxed under anhydrous conditions for 12−14 h, cooled to room temperature, filtered, and ethanol was recovered under vacuum resulting in a white crude product. The white crude product so obtained was dissolved in dichloromethane/diethyl ether and washed with brine four to five times. The organic layer was separated, dried over anhydrous sodium sulfate, and recovered to obtain the desired tertiary amine (**6IV**) as a yellowish colored waxy solid (13 g, 90%) (mp 60−62 °C). TLC: R_f 0.7 (10% MeOH in $CHCl_3$). IR: 3377, 1150, 1043 cm^{-1}.

4.3.1.2. Method-B: Preparation of the Targeted GAs. 1,4-Di[(*n*-hexadecyldimethylammonium)methyl]benzene dibromide (**9AI**): the title compound was prepared from *N*-hexadecyl-*N*,*N*-dimethylamine (**1**) (2.96 mL, 8.8 mmol) and dibromo-*p*-xylene (**7**) (1.04 g, 4.0 mmol) in dry acetone. The reaction mixture was taken in a sealed tube and heated at ∼80 °C for 2−3 days resulting in a white precipitate. After removing the solvent, the obtained residue was washed with diethyl ether. The crude so obtained was recrystallized three to four times using a mixture of methanol and ethyl acetate to afford the title product (**9AI**) as a white solid (2.2 g, 70%) (mp 237−39 °C). TLC: 0.5 (10% MeOH in $CHCl_3$). IR: 3126, 1097 cm^{-1}. PMR: δ 0.87 (t, 6H), 1.25−1.36 (bm, 52H), 1.67−1.85 (bm, 4H), 3.22 (s, 12H), 3.55 (t, 4H), 5.36 (s, 4H), 7.80 (s, 4H). Anal. calcd for $C_{44}H_{86}N_2Br_2$, C, 65.81; H, 10.80; N, 3.49; found, C, 65.58; H, 11.12; N, 3.32%.

1,4-Di{[*n*-hexadecyl(2-hydroxyethyl)methylammonium]-methyl}benzene dibromide (**9BI**): the title compound was prepared from *N*-hexadecyl-*N*-methylethanolamine (**5I**) (2.64 g, 8.8 mmol) and dibromo-*p*-xylene(7) (1.04 g, 4.0 mmol) following Method-B to afford the product (**9BI**) as a white solid (2.0 g, 60%) (mp 217−19 °C). TLC/R_f 0.35 (10% MeOH in $CHCl_3$). IR: 3310, 2997, 1099, 1048 cm^{-1}. PMR: δ 0.85 (t, 6H), 1.22 (bm, 52H), 1.77−2.08 (m, 4H), 2.96 (s, 6H), 3.30 (bt, 8H), 3.88 (t, 4H), 4.63 (t, 4H), 5.35 (br s, 2H), 7.67 (s, 4H). Anal. calcd for $C_{46}H_{90}N_2O_2Br_2$, C, 64.02; H, 10.51; N, 3.25; found, C, 63.83; H, 10.73; N, 3.47%.

1,4-Di{[*n*-dodecyl(2-hydroxyethyl)methylammonium]-methyl}benzene dibromide (**9BII**): the title compound was prepared from *N*-dodecyl-*N*-methylethanolamine (**5II**) (2.16 g, 8.8 mmol) and dibromo-*p*-xylene (**7**) (1.04 g, 4.0 mmol) as per Method-B to obtain a precipitate, which was washed with diethylether. The crude product so obtained was recrystallized three to four times using a mixture of methanol and ethylacetate to afford the title product (**9BII**) as a white solid (1.8 g, 64%) (mp 216−18 °C). TLC: R_f 0.3 (10% MeOH in $CHCl_3$). IR: 3311, 1472, 1099, 1038 cm^{-1}. PMR: δ 0.59 (t, 6H), 0.99 (bm, 36H), 1.53 (m, 4H), 2.72 (s, 6H), 3.076 (t, 4H), 3.173−3.214 (t, 4H), 3.649 (t, 4H), 4.404 (t, 4H), 5.121 (br s, 2H), 7.431 (s, 4H). Anal. calcd for $C_{38}H_{74}N_2O_2Br_2$, C, 60.79; H, 9.93; N, 3.73; found, C, 60.62; H, 10.11; N, 3.95%.

1,4-Di{[(2-hydroxyethyl)methyl-*n*-tetradecylammonium]-methyl}benzene dibromide (**9BIII**): the title compound was prepared from *N*-tetradecyl-*N*-methyl-2-hydroxyethylamine (**5III**) (2.40 g, 8.8 mmol) and dibromo-*p*-xylene (**7**) (1.04 g, 4.0 mmol) following the method described for synthesis of compound (**7aI**) to afford the product (**9BIII**) as a white solid (2.1 g, 67%) (mp 217−19 °C). TLC/R_f 0.3 (10% MeOH in $CHCl_3$). IR: 3312, 2994, 1102, 1050 cm^{-1}. PMR: δ 0.88 (t, 6H), 1.25−1.35 (bm, 44H), 1.81 (m, 4H), 3.20 (s, 6H), 3.42 (t, 4H), 3.58 (bm, 8H), 4.14 (t, 4H), 5.08 (br s, 2H), 7.77 (s, 4H). Anal. calcd for $C_{42}H_{82}N_2O_2Br_2$, C, 62.52; H, 10.24; N, 3.47; found, C, 62.39; H, 10.53; N, 3.25%.

1,4-Di{[(2-hydroxyethyl)methyl-*n*-octadecylammonium]-methyl}benzene dibromide (**9BIV**): the title compound was prepared from *N*-methyl-*N*-octadecylethanolamine (**5IV**) (2.88 g, 8.8 mmol) and dibromo-*p*-xylene (**7**) (1.04 g, 4.0 mmol) following Method-B to afford the product (**9BIV**) as a white solid (2.3 g, 66%) (mp 218−20 °C). TLC/R_f 0.4 (10% MeOH in $CHCl_3$). IR: 3312, 2997, 1099, 1049 cm^{-1}. PMR: δ 0.85 (t, 6H), 1.25−1.37 (bm, 60H), 1.67 (m, 4H), 3.20 (s, 6H), 3.58−3.60 (bt, 8H), 4.09 (t, 4H), 4.90 (t, 4H), 5.30 (br s, 2H), 7.8 (s, 4H). Anal. calcd for $C_{50}H_{98}N_2O_2Br_2$, C, 65.34; H, 10.75; N, 3.05; found, C, 62.16; H, 10.96; N, 2.88%.

1,4-Di{[*n*-hexadecyldi(2-dihydroxyethyl)ammonium]-methyl}benzene dibromide (**9CI**): the title compound was prepared from *N*,*N*-di(2-hydroxyethyl)-*N*-hexadecylamine (**6I**) (2.92 g, 8.8 mmol) and dibromo-*p*-xylene (**7**) (1.04 g, 4.0 mmol) following Method-B to afford the desired

https://doi.org/10.1021/acsomega.1c03667
ACS Omega 2021, 6, 33370−33388

compound (**9CI**) as a white solid (2.5 g, 62%) (mp 210−12 °C).TLC/R_f 0.3 (10% MeOH in $CHCl_3$). IR: 3384, 3108, 1096, 1049 cm^{-1}. PMR: δ 0.83 (t, 6H), 1.22 (bm, 52H), 1.81 (m, 4H), 3.20 (t, 4H), 3.31 (bt, 8H), 3.92 (t, 8H), 4.72 (s, 4H), 5.38 (br s, 4H), 7.67 (s, 4H). Anal. calcd for $C_{48}H_{94}N_2O_4Br_2$, C, 62.46; H, 10.26; N, 3.03; found, C, 62.19; H, 10.53; N, 2.76%.

1,4-Di{[*n*-dodecyldi(2-dihydroxyethyl)ammonium]methyl}-benzene dibromide (**9CII**): the title compound was prepared from *N*-dodecyl-*N*,*N*-di(2-hydroxyethyl)amine (**6II**) (2.4 g, 8.8 mmol) and dibromo-*p*-xylene (**7**) (1.04 g, 4.0 mmol) using Method-B to obtain a crude product. The crude so obtained was recrystallized three to four times using a mixture of methanol and ethyl acetate to afford the product (**9CII**) as a white solid (1.9 g, 65%) (208−10 °C). TLC: 0.25 (10% MeOH in $CHCl_3$). IR: 3409, 3114, 1099, 1046 cm^{-1}. PMR: δ 0.924 (t, 6H), 1.319 (bm, 36H), 1.877 (m, 4H), 3.301 (t, 4H), 3.402−3.444 (bt, 4H), 4.005 (bt, 8H), 4.813 (s, 4H), 5.466 (br s, 4H), 7.762 (s, 4H). Anal. calcd for $C_{40}H_{78}N_2O_4Br_2$, C, 59.25; H, 9.70; N, 3.45; found, C, 59.04; H, 9.97; N, 3.09%.

1,4-Di{[di(2-dihydroxyethyl)-*n*-tetradecyl-ammonium]-methyl}benzene dibromide (**9CIII**): the title compound was prepared from *N*,*N*-di(2-hydroxyethyl)-*N*-tetradecylamine (**6III**) (2.64 g, 8.8 mmol) and dibromo-*p*-xylene (**7**) (1.04 g, 4.0 mmol) following Method-B to afford the desired product (**9CIII**) as a white solid (2.2 g, 66%) (mp 207−09 °C). TLC/R_f 0.3 (10% MeOH in $CHCl_3$). IR: 3388, 3109, 1099, 1047 cm^{-1}. PMR: δ 0.85 (t, 6H), 1.25 (bm, 44H), 1.80 (m, 4H), 3.39 (t, 8H), 3.92 (bt, 8H), 4.74 (bt, 8H), 5.36 (br s, 4H), 7.69 (s, 4H). Anal. calcd for $C_{44}H_{86}N_2O_4Br_2$, C, 60.96; H, 10.00; N, 3.23; found, C, 60.62; H, 10.32; N, 3.07%.

1,4-Di{[di(2-hydroxyethyl)-*n*-octadecylammonium]-methyl}benzene dibromide (**9CIV**): the title compound was prepared from *N*,*N*-di(2-hydroxyethyl)-*N*-octadecylamine (**6IV**) (3.16 g, 8.8 mmol) and dibromo-*p*-xylene (**7**) (1.04 g, 4.0 mmol) following Method-B to afford the desired compound (**9CIV**) as a white solid (2.6 g, 69%) (mp 224−26 °C). TLC/R_f 0.5 (10% MeOH in $CHCl_3$). IR: 3313, 1096, 1049 cm^{-1}. PMR: δ 0.85 (t, 6H), 1.23 (bm, 60H), 1.78 (m, 4H), 3.12−3.33 (bm, 16H), 3.91−4.64 (bt, 8H), 7.67 (br s, 4H). Anal. calcd for $C_{52}H_{102}N_2O_4Br_2$, C, 63.78; H, 10.50; N, 2.86; found, C, 63.51; H, 10.85; N, 2.71%.

2,2′-Di(*n*-hexadecyldimethylammoniumethyl)ether dibromide (**10AI**): the title compound was prepared from *N*-hexadecyl-*N*,*N*-dimethylamine (**1**) (2.96 mL, 8.8 mmol) and 2,2′-dibromodiethyl ether (**8**) (0.51 mL, 4.0 mmol) following Method-B to afford a white solid compound (**10AI**) (2.0 g, 67%), (mp 243−45 °C). TLC: 0.4 (10% MeOH in $CHCl_3$). IR: 1139, 1082, 973 cm^{-1}. PMR: δ 0.88 (t, 6H), 1.25−1.35 (bm, 52H), 1.72 (bm, 4H), 3.44 (s, 12H), 3.58−3.63 (t, 4H), 4.07 (br s, 4H), 4.33 (br s, 4H). Anal. calcd for $C_{40}H_{86}N_2OBr_2$, C, 62.32; H, 11.24; N, 3.63; found, C, 62.09; H, 11.57; N, 3.38%.

2,2′-Di[*n*-hexadecyl(2-hydroxyethyl)-methylammoniumethyl]ether dibromide (**10BI**): the title compound was prepared from *N*-hexadecyl-*N*-methylethanolamine (**5I**) (2.64 g, 8.8 mmol) and 2,2′-dibromodiethyl ether (**8**) (0.51 mL, 4.0 mmol) following Method-B to afford the product (**10BI**) as a white solid (2.2 g, 66%) (mp 227−29 °C). TLC/R_f 0.35 (10% MeOH in $CHCl_3$). IR: 3322, 1132, 1082, 1049 cm^{-1}. PMR: δ 0.88 (t, 6H), 1.25−1.34 (bm, 52H), 1.71 (m, 4H), 2.08 (t, 4H), 3.39 (s, 6H), 3.62 (t, 4H), 3.81 (t, 4H), 4.09 (t, 4H), 4.25 (t, 4H), 4.98 (br s, 2H). Anal. calcd for $C_{42}H_{90}N_2O_3Br_2$, C, 60.71; H, 10.92; N, 3.37; found, C, 60.49; H, 11.26; N, 3.08%.

2,2′-Di[*n*-dodecyl(2-hydroxyethyl)methylammoniumethyl]-ether dibromide (**10BII**): the title compound was prepared from *N*-dodecyl-*N*-methylethanolamine (**5II**) (2.16 g, 8.8 mmol) and 2,2′-dibromodiethylether (**8**) (0.51 mL, 4.0 mmol) following Method-B to afford the desired product (**10BII**) as a white solid (1.6 g, 58%) (mp 215−18 °C).TLC/R_f 0.3 (10% MeOH in $CHCl_3$). IR: 3334, 1129, 1082, 1049 cm^{-1}. PMR: δ 0.85 (t, 6H), 1.25−1.34 (bm, 36H), 1.72 (m, 4H), 3.39 (s, 6H), 3.63 (t, 4H), 3.81 (t, 4H), 3.97 (t, 4H), 4.10 (t, 4H), 4.25 (t, 4H), 4.95 (br s, 2H). Anal. calcd for $C_{34}H_{74}N_2O_3Br_2$, C, 56.81; H, 10.38; N, 3.90; found, C, 56.53; H, 10.67; N, 3.61%.

2,2′-Di[(2-hydroxyethyl)methyl-*n*-tetradecylammonium-ethyl]ether dibromide (**10BIII**): the title compound was prepared from *N*-methyl-*N*-tetradecylethanolamine (**5III**) (2.40 g, 8.8 mmol) and 2,2′-dibromodiethyl ether (**8**) (0.51 mL, 4.0 mmol) following Method-B to afford the quaternary product (**10BIII**) as a white solid (1.8 g, 60%) (mp 234−36 °C).TLC/R_f 0.3 (10% MeOH in $CHCl_3$). IR: 3290, 1132, 1082, 1049 cm^{-1}. PMR: δ 0.85 (t, 6H), 1.25−1.34 (bm, 44H), 1.71−2.07 (m, 4H), 3.39 (s, 6H), 3.63 (t, 4H), 3.81 (t, 4H), 3.98 (t, 4H), 4.10 (t, 4H), 4.25 (t, 4H), 4.97 (br s, 2H). Anal. calcd for $C_{38}H_{82}N_2O_3Br_2$, C, 58.90; H, 10.67; N, 3.62; found, C, 58.68; H, 10.92; N, 3.44%.

2,2′-Di[(2-hydroxyethyl)methyl-*n*-octadecylammonium-ethyl]ether dibromide (**10BIV**): the title compound was prepared from *N*-methyl-*N*-octadecylethanolamine (**5IV**) (2.88 g, 8.8 mmol) and 2,2′-dibromodiethyl ether (**8**) (0.51 mL, 4.0 mmol) following Method-B to afford (**10BIV**) as a white solid (2.0 g, 56%) (mp 224−26 °C). TLC/R_f 0.4 (10% MeOH in $CHCl_3$). IR: 3323, 1132, 1082, 1049 cm^{-1}. PMR: δ 0.85 (t, 6H), 1.25−1.35 (bm, 60H), 1.71 (m, 4H), 1.99 (t, 4H), 3.39 (s, 6H), 3.63 (t, 4H), 3.81 (t, 4H), 4.10 (t, 4H), 4.26 (t, 4H), 4.95 (br s, 2H). Anal. calcd for $C_{46}H_{98}N_2O_3Br_2$, C, 62.28; H, 11.14; N, 3.16; found, C, 61.81; H, 11.46; N, 2.87%.

2,2′-Di[di(2-dihydroxyethyl)-*n*-tetradecylammoniumethyl]-ether dibromide (**10CIII**): the title compound was prepared from *N*,*N*-di(2-hydroxyethyl)-*N*-tetradecylamine (**6III**) (2.64 g, 8.8 mmol) and 2,2′-dibromodiethylether (**8**) (0.51 mL, 4.0 mmol) following Method-B to afford the desired product (**10CIII**) as a white solid (2.1 g, 62%) (mp 218−20). TLC: 0.3 (10% MeOH in $CHCl_3$). IR: 3300, 1103, 1076, 978 cm^{-1}. PMR: δ 0.85 (t, 6H), 1.22 (bm, 44H), 1.71 (bt, 4H), 3.59 (t, 4H), 3.78−3.91 (bm, 12H), 4.08−4.17 (bm, 12H), 4.82 (br s, 4H). Anal. calcd for $C_{40}H_{86}N_2O_5Br_2$, C, 57.54; H, 10.38; N, 3.36; found, C, 57.25; H, 10.77; N, 3.02%.

2,2′-Di[di(2-dihydroxyethyl)-*n*-octadecylammoniumethyl]-ether dibromide (**10CIV**): the title compound was prepared from *N*,*N*-di(2-hydroxyethyl)-*N*-octadecylamine (**6IV**) (3.16 g, 8.8 mmol) and 2,2′-dibromodiethylether (**8**) (0.51 mL, 4.0 mmol) following Method-B to afford the desired compound (**10CIV**) as a white solid (2.1 g, 56%) (mp 226−28 °C). TLC: 0.5 (10% MeOH in $CHCl_3$). IR: 3300, 1105, 1074, 978 cm^{-1}. PMR: δ 0.85 (t, 6H), 1.23−1.65 (bm, 60H), 3.27−3.37 (bt, 8H), 3.49 (t, 8H), 3.64 (bm, 4H), 3.80 (bm, 12H), 5.28 (br s, 4H). Anal. calcd for $C_{48}H_{102}N_2O_5Br_2$, C, 60.87; H, 10.85; N, 2.96; found, C, 60.53; H, 11.22; N, 2.68%.

4.4. CMC Determination. Aqueous solutions of the GAs were prepared in the range of 10^{-3} to 10^{-6} mmol for all GAs. Specific conductance of these solutions was determined using a digital conductometer (Equiptronics, model 306, Mumbai)

https://doi.org/10.1021/acsomega.1c03667
ACS Omega 2021, 6, 33370−33388

with a cell constant of 1.01 S cm^{-1} at 30 ± 0.2 °C. Specific conductance was plotted against the concentration of the GA solutions. Inflexion point indicated the formation of micelles in the solutions offering the cmc of the GAs.[57]

4.5. Preparation of GA Liposomal Formulations. Formulations were prepared using each GA alone and in combination with helper lipid DOPE. Both GA and DOPE in molar ratios of 1:1 (Formulation a), 1:2 (Formulation b), and 1:3 (Formulation c) were dissolved in a solvent mixture (chloroform/methanol, 1:1) in glass vials in such a way that the total lipid contents remained constant. A nitrogen stream was passed over the solution to remove the organic solvents. For removal of residual amounts of solvent, the samples were further maintained overnight under high vacuum. HEPES buffer (20 mM, pH 7.4) was used for hydrating the dry film and the resulting mixture was incubated at about 70 °C for 30 min. After incubation, the hot mixture was subjected to many cycles of vigorous vortexing and cooling in a cold bath and again heating to about 70 °C to ensure proper hydration of the film. The suspension so obtained was finally sonicated for 3 min and filtered two to three times through a polycarbonate filter (0.22 μm). DOTAP−DOPE and DCC−DOPE formulations as the standard liposomal formulations were also prepared in the same way. Some formulations containing cholesterol as a helper lipid along with DOPE were also prepared so that the final formulations contained GA/DOPE/cholesterol[58] in molar ratios of 1:1:1 (Formulation d) and 1:1:0.5 (Formulation e).

4.6. Lipoplex Preparation Using the Reporter pDNA. Freshly prepared GA liposomal formulations were used for preparing pDNA lipoplexes by vortexing them with pDNA in DMEM in different N/P ratios (0.5 to 6.0). The N/P ratio is defined as the ratio of nitrogen contents present in the GA to phosphorous contents present in the pDNA. The quantity of pDNA was kept constant and the quantity of the GA formulation was changed to achieve the required N/P ratio. However, the volume of the liposomal formulation and the dilution of the pDNA were kept constant for lipoplex preparation. In a typical setup, different amounts of the GA formulations were used to obtain different N/P ratios in a HEPES buffer (30 μL, pH 7.4) and these were treated with pDNA (1 μg) and incubated for 30 min at room temperature on a rotary shaker. The lipoplexes so obtained were used for characterization and for other studies immediately after their preparation.[59]

4.7. Size and Zeta Potential Determination of the Liposomal and Polyplex Formulations. A Malvern Zetasizer Nano (Malvern Instruments, UK) was used for the determination of the particle size (*z*-average) and PDI of the formulations.[60] Photon correlation spectroscopy is a non-invasive back-scatter technique on which the Zetasizer Nano works at 4 mW using a helium−neon laser at 633 nm at a temperature of 25 °C. Measurements were performed in manual mode for 20 subruns of 10 s each. The size distribution was calculated using Dispersion Technology Software (version 4.0, Malvern, Herrenberg, Germany). The measurement of electrophoretic mobility (μm/s) was done using a small volume disposable zeta cell, which was converted to zeta potential using in-built software working on the principle of the Helmholtz−Smoluchowski equation. The liposomes and lipoplexes (0.2 mL) of GAs were diluted to 1.0 mL with DMEM for the measurement of size and zeta potential.

For TEM, a drop of the lipoplex was applied to the copper grid; excess of the preparation was removed with the help of a filter paper and allowed to dry. An aqueous solution (2%) of uranyl acetate was applied to the complex. Excess of the solution was again removed with the help of a filter paper, allowed to dry, and the grid was subjected to electron microscopy.[60]

4.8. Agarose Gel Retardation Assay for pDNA Complexation. In order to evaluate the DNA-binding ability of the GAs, the gel retardation assay was used. For this purpose, agarose gel (1%) prestained with ethidium bromide (0.1%) was used. The reporter pDNA (300 ng) was complexed with the GA liposomal formulations in different N/P ratios (0.25, 0.5, 0.75, 1, 1.5, 2, 3, 4, and 6) in HEPES buffer (pH 7.4) in a total volume of 20 μL by incubation for 20−25 min at room temperature. Loading buffer was prepared by mixing bromophenol blue (0.25%) in aqueous solution of sucrose (40%), and 4 L of the loading buffer was added in each well. Electrophoresis was performed with Tris acetate buffer for 40 min at 80 V. The DNA bands were visualized using the gel documentation unit.[48]

4.9. Evaluation of pDNA Protection in the Lipoplexes. Lipoplexes having different N/P ratios of the GA/pDNA but having a fix quantity of pDNA were incubated with DNase I enzyme (1 μg/mL, 10 μL) at 37 °C for 20 min in the presence of magnesium chloride (20 mM). After the given time, the enzymatic reaction was stopped by adding EDTA (50 mM), the mixture was further incubated for 10 min at 60 °C, the aqueous layer was washed with a phenol/chloroform/isoamyl alcohol (25:24:1 v/v) mixture, and centrifuged for 5 min at 10,000 rpm. The aqueous supernatant (25 μL) containing the pDNA was applied on agarose gel (1%), which was prestained with ethidium bromide, electrophoresed for 1 h at 100 V,[48] and visualized under the gel documentation unit.

4.10. CD Study for pDNA Condensation. In order to find out any conformational change, which could take place in the pDNA after complexation with the GAs at different N/P ratios, CD spectroscopy of the lipoplexes was carried out on a JASCO-J815 instrument in the wavelength range of 320−200 nm. The sample was held in a quartz cuvette with a 0.2 cm cell length, and scanning was performed at a speed of 50 nm/min at a band width of 1 nm.[61] The native form of pDNA without complexation or in the absence of the GAs elicits a positive band at 277 nm and a negative band at 245 nm indicating the existence of B-form of the DNA.[62]

4.11. Transfection Studies Using the Reporter Gene.

4.11.1. Transfection Studies in the Absence of Serum. In order to evaluate the transfection efficacy of the GAs, formulations [i.e., lipoplexes formed with the pDNA (i.e., the reporter gene p*CMV*.SPORT-*β-gal*) (300 ng) using the GAs all alone or in combination with the helper lipid DOPE] containing the GAs in different N/P ratios (1 to 6) were used for transfecting two cell lines A549 and HeLa in modified DMEM (containing 10% FBS).[36,63−65] The method is explicitly described in our earlier publication.[44] The intensity of the yellow color of formed *p*-nitrophenol was measured at 405 nm using an ELISA plate reader (BIorad, model 680XR, Mumbai, India). The color intensity is directly proportional to the transfection efficacy of the GA formulation.

4.11.2. Transfection of Cells in the Presence of Serum. To check the transfection efficacy of the GA formulation in the presence of serum, additional FBS (10%) was added in the medium while inoculating the cells with the lipoplex

https://doi.org/10.1021/acsomega.1c03667
ACS Omega 2021, 6, 33370−33388

formulations, maintaining the rest of the conditions the same as reported in Section 4.11.1.

4.12. FACS Studies. FACS studies were performed as reported earlier.[44] Cells were seeded in DMEM growth medium (1 mL) containing the antibiotic cocktail of penicillin−streptomycin−amphotericin B (1%) and FBS (10%) in 24-well plates containing 50,000 cells/well. After a lag period of 18−24 h, lipoplex treatment was given to the cells in plain DMEM (500 μL). The culture medium was removed from the wells after 4 h of incubation with the lipoplexes, and the wells were washed with PBS (pH 7.4). Fresh growth medium (1 mL) was added to each well and the cells were analyzed using the protocol for FACS in the absence of light to avoid fluorescence quenching.[66]

Transfection was analyzed in wells after 48 h using a fluorescence microscope (Nikon). Media were aspirated from all the wells into microcentrifuge tubes. Each well was washed with 100 μL of 1X PBS and aspirated into respective microcentrifuge tubes. Each well was treated with Trypsin−EDTA (250 μL) and incubated for 5−10 min at 37 °C. Detachment of cells in each well was observed under a microscope and complete media (100 μL) were added to each well. The media were aspirated into microcentrifuge tubes from each well and centrifuged to 8000 rpm at 4 °C for 10 min. Filtrates were discarded and pellets were resuspended in 1× PBS (500 μL), washed with PBS, and then centrifuged again under aforementioned conditions. Filtrates were discarded and 1× PBS (500 μL) was added to each microcentrifuge tube. Paraformaldehyde (500 μL, 8%) was added to each microcentrifuge tube and left for 5−10 min to fix the cells and centrifuged under aforementioned conditions. Supernatants were discarded and tubes were washed with 1× PBS (500 μL) and centrifuged under same conditions to remove paraformaldehyde completely. Filtrates were discarded again and pellets were finally resuspended in 1× PBS (500 μL) to obtain the samples ready for FACS reading. The presence of GFP was detected by emission at a wavelength of 508 nm using a flow cytometer (Guava Easycyte; Guava Technologies Inc.). For each cell sample, 5000 events were collected.

4.13. Confocal Microscopy. For evaluating intracellular trafficking of the lipoplexes obtained from the GA formulation (**10BIIId**), confocal microscopy was performed as described earlier.[44] HeLa cells were cultured in 6-well plates (2 × 105 cells per well) in the growth media and transfected with the lipoplex (of **10BIIId**). After predetermined time intervals, each well was washed with PBS (3 × 1 mL), the cells were fixed with 4% paraformaldehyde solution (1 mL) for 10 min, and the excess of paraformaldehyde was removed by washing with PBS (3 × 1 mL). Finally, cells were treated with nuclear staining dye DAPI (0.7 mL) for an hour and excess of the dye was washed again with PBS (3 × 1 mL). Cells were viewed under a confocal microscope (Zeiss, LSM-510 META, Germany) at a 520 nm emission wave length and an excitation wavelength of 488 nm.

4.14. MTT Assay for Cytotoxicity Evaluation. Cytotoxicity tests for the GA formulations were performed using the 3-(4,5-dimethylthiazol-2-yl)-2,5-diphenyltetrazolium bromide (MTT) reduction assay as reported in our earlier publication.[44] The ratio of the number of cells to the quantity of GAs present in the formulations was maintained the same in the MTT assay in 96-well plates, as maintained in the assays performed for evaluating the transfection efficacy of the GA formulations. The cells were incubated with the formulations for 4 h after which the media were removed, and the wells were washed with 7.4 pH buffer solution and 200 μL of fresh culture medium was added. After 48 h of incubation, the culture medium was again removed and the wells were again washed with the buffer solution. The cells were then incubated for 4 h at 37 °C with MTT solution (50 μL) containing 1 mg/mL of the MTT reagent in plain DMEM. After removal of the DMEM, 100 μL of DMSO was added to each well to dissolve the formazan crystals formed by reduction of the MTT reagent by the living cells. Absorbance was determined at 570 nm on an ELISA plate reader by fixing the reference at 650 nm and % viability of the cells was determined by applying the given formula[67,68]

$$\%\ \text{cell viability} = \frac{\text{absorbance of sample}}{\text{absorbance of control}} \times 100$$

4.15. In Vivo Animal Studies. *4.15.1. Optimization of Radiolabeling Lipoplexes by the Direct Labeling Procedure.* The procedure adopted for performing radiolabeling of the GA lipoplexes with ^{99m}Tc has been taken from our earlier publication.[44] Freshly prepared lipoplexes of the GAs with the pDNA (15 μg) were treated with sodium pertechnetate (^{99m}Tc), followed by treatment with stannous chloride (1 mg/mL, 0.1 mL) in saline solution maintaining the pH 6.0−6.5 with the help of sodium bicarbonate buffer (0.5 M, pH 9.0) to obtain a radioactivity level of 2.5 mCi/mL. Radiolabeling efficiency of the labeling reagent and the purity level of the labeled lipoplexes were checked using the ITLC technique. The procedure was standardized by varying parameters such as the concentration of the labeling reagent, concentration of the reducing agent stannous chloride, pH of the medium, and other related parameters to obtain stable radio-labeled lipoplexes.

4.15.2. Biodistribution Studies. The method reported[44] earlier was followed. Approval was obtained by the local IAEC, Institute of Nuclear Medicine and Allied Science, New Delhi. The radiolabeled (^{99m}Tc) lipoplex of the GA formulation (**10BIIId**) was parenterally injected (0.2 mL per animal) into Balb/C mice through tail vein. At different time intervals, the blood sample was withdrawn by cardiac puncture and organs were harvested by sacrificing the animals by cervical dislocation. The tissues were washed with normal saline, soaked free from fluid/saline by tissue paper, weighed, and the radioactivity was measured using a well-type shielded γ-scintillation counter (Electronics Corporation of India, Mumbai make). Three animals were used for each time point. The percentage of radioactivity present per gram of the tissue was calculated using the equation[69]

$$\%\ \text{radioactivity/g of tissue} = \frac{\text{radioactivity count of the tissue}}{\text{weight of the tissue} \times \text{total count injected}} \times 100$$

■ ASSOCIATED CONTENT

Supporting Information

The Supporting Information is available free of charge at https://pubs.acs.org/doi/10.1021/acsomega.1c03667.

Representative plot for cmc determination of GAs: cmc values obtained for the synthesized GAs; CD spectra; transfection efficacies; percent cell viability; and PMR spectrum (PDF)

https://doi.org/10.1021/acsomega.1c03667
ACS Omega 2021, 6, 33370−33388

AUTHOR INFORMATION

Corresponding Author

Mange Ram Yadav − *Faculty of Pharmacy, The Maharaja Sayajirao University of Baroda, Vadodara 390 001 Gujarat, India; Centre of Research for Development, Parul University, Vadodara 391 760 Gujarat, India;* orcid.org/0000-0003-2020-5225; Email: mryadav11@yahoo.co.in

Authors

Mukesh Kumar − *Faculty of Pharmacy, The Maharaja Sayajirao University of Baroda, Vadodara 390 001 Gujarat, India*

Prashant R. Murumkar − *Faculty of Pharmacy, The Maharaja Sayajirao University of Baroda, Vadodara 390 001 Gujarat, India*

Complete contact information is available at: https://pubs.acs.org/10.1021/acsomega.1c03667

Notes

The authors declare no competing financial interest.

ACKNOWLEDGMENTS

The authors express their gratitude to Dr Pradeep Kumar, Scientist, Nucleic Acid Chemistry, Institute of Genomics and Integrative Biology, New Delhi, for providing permission to use facilities to perform FACS and confocal studies. The authors are also thankful to Dr Anil K. Mishra, Division of Radiopharmaceuticals, Institute of Nuclear Medicine & Allied Sciences (INMAS), Delhi, for carrying out the radiolabeling studies. M.R.Y. is thankful to UGC, New Delhi, for awarding the UGC-BSR Faculty Fellowship [no. F.18-1/2011(BSR)].

REFERENCES

(1) Walsh, C. E. Gene therapy progress and prospects: Gene therapy for the hemophilias. *Gene Ther.* **2003**, *10*, 999−1003.

(2) Hazan-Halevy, I.; Landesman-Milo, D.; Rosenblum, D.; Mizrahy, S.; Ng, B. D.; Peer, D. Immunomodulation of hematological malignancies using oligonucleotides based-nanomedicines. *J. Controlled Release* **2016**, *244*, 149−156.

(3) Nabel, E. Gene therapy for cardiovascular diseases. *J. Nucl. Cardiol.* **1999**, *6*, 69−75.

(4) Landmesser, U.; Poller, W.; Tsimikas, S.; Most, P.; Paneni, F.; Lüscher, T. F. From traditional pharmacological towards nucleic acid-based therapies for cardiovascular diseases. *Eur. Heart J.* **2020**, *41*, 3884−3899.

(5) Nielsen, T.; Nielsen, J. Antisense gene silencing: Therapy for neurodegenerative disorders? *Genes* **2013**, *4*, 457−484.

(6) Burton, E. A.; Glorioso, J. C.; Fink, D. J. Gene therapy progress and prospects: Parkinson's disease. *Gene Ther.* **2003**, *10*, 1721−1727.

(7) Alisky, J. M.; Davidson, B. L. Gene therapy for amyotrophic lateral sclerosis and other motor neuron diseases. *Hum. Gene Ther.* **2000**, *11*, 2315−2329.

(8) Winkelsas, A. M.; Fischbeck, K. H. Nucleic acid therapeutics in neurodevelopmental disease. *Curr. Opin. Genet. Dev.* **2020**, *65*, 112−116.

(9) Amer, M. H. Gene therapy for cancer: present status and future perspective. *Mol. Cell. Ther.* **2014**, *2*, 27.

(10) Parsel, S. M.; Grandis, J. R.; Thomas, S. M. Nucleic acid targeting: Towards personalized therapy for head and neck cancer. *Oncogene* **2016**, *35*, 3217−3226.

(11) Roberts, T. C.; Langer, R.; Wood, M. J. A. Advances in oligonucleotide drug delivery. *Nat. Rev. Drug Discovery* **2020**, *19*, 673−694.

(12) Adams, D.; Gonzalez-Duarte, A.; O'Riordan, W. D.; Yang, C.-C.; Ueda, M.; Kristen, A. V.; Tournev, I.; Schmidt, H. H.; Coelho, T.; Berk, J. L.; Lin, K.-P.; Vita, G.; Attarian, S.; Planté-Bordeneuve, V.; Mezei, M. M.; Campistol, J. M.; Buades, J.; Brannagan, T. H.; Kim, B. J.; Oh, J.; Parman, Y.; Sekijima, Y.; Hawkins, P. N.; Solomon, S. D.; Polydefkis, M. P.; Dyck, P. J.; Gandhi, P. J.; Goyal, S.; Chen, J.; Strahs, A. L.; Nochur, S. V.; Sweetser, M. T.; Garg, P. P.; Vaishnaw, A. K.; Gollob, J. A.; Suhr, O. B. Patisiran, an RNAi Therapeutic, for Hereditary Transthyretin Amyloidosis. *N. Engl. J. Med.* **2018**, *379*, 11−21.

(13) Scott, L. J. Givosiran: First Approval. *Drugs* **2020**, *80*, 335−339.

(14) FDA News Release. *FDA Approves First Drug to Treat Rare Metabolic Disorder*; FDA, 2020.

(15) FDA News Release. *FDA grants accelerated approval to first targeted treatment for rare Duchenne muscular dystrophy mutation*; FDA, 2019.

(16) IONIS press release. *Akcea and Ionis Receive FDA Approval of TEGSEDITM (inotersen) for the Treatment of the Polyneuropathy of Hereditary Transthyretin-Mediated Amyloidosis in Adults*; IONIS, 2018.

(17) FDA News Release. *FDA approves first drug for spinal muscular atrophy*; FDA, 2016.

(18) FDA News Release. *FDA grants accelerated approval to first drug for Duchenne muscular dystrophy*; FDA, 2016.

(19) FDA News Release. *FDA approves first treatment for rare disease in patients who receive stem cell transplant from blood or bone marrow*; FDA, 2016.

(20) Hair, P.; Cameron, F.; McKeage, K. Mipomersen sodium: First global approval. *Drugs* **2013**, *73*, 487−493.

(21) Highleyman, L. *FDA approves fomivirsen, famciclovir, and Thalidomide*; BETA, 1998; p 5.

(22) Doggrell, S. A. Pegaptanib: The first antiangiogenic agent approved for neovascular macular degeneration. *Expert Opin. Pharmacother.* **2005**, *6*, 1421−1423.

(23) FDA News Release. *Pfizer-BioNTech COVID-19 Vaccine FDA*; FDA, 2020.

(24) FDA News Release. *Moderna COVID-19 Vaccine FDA*; FDA,2020.

(25) Ledley, F. D. Pharmaceutical approach to somatic gene therapy. *Pharm. Res.* **1996**, *13*, 1595−1614.

(26) Vacik, J.; Dean, B. S.; Zimmer, W. E.; Dean, D. A. Cell-specific nuclear import of plasmid DNA. *Gene Ther.* **1999**, *6*, 1006−1014.

(27) Schaffer, D. V.; Lauffenburger, D. A. Optimization of cell surface binding enhances efficiency and specificity of molecular conjugate gene delivery. *J. Biol. Chem.* **1998**, *273*, 28004−28009.

(28) Ginn, S. L.; Alexander, I. E.; Edelstein, M. L.; Abedi, M. R.; Wixon, J. Gene therapy clinical trials worldwide to 2012 - an update. *J. Gene Med.* **2013**, *15*, 65−77.

(29) Han, S.-o.; Mahato, R. I.; Sung, Y. K.; Kim, S. W. Development of biomaterials for gene therapy. *Mol. Ther.* **2000**, *2*, 302−317.

(30) Cotten, M.; Wagner, E. Non-viral approaches to gene therapy. *Curr. Opin. Biotechnol.* **1993**, *4*, 705−710.

(31) Gao, X.; Kim, K.-S.; Liu, D. Nonviral gene delivery: what we know and what is next. *AAPS J.* **2007**, *9*, E92−E104.

(32) Yang, Y.; Nunes, F. A.; Berencsi, K.; Gönczöl, E.; Engelhardt, J. F.; Wilson, J. M. Inactivation of E2a in recombinant adenoviruses improves the prospect for gene therapy in cystic fibrosis. *Nat. Genet.* **1994**, *7*, 362−369.

(33) Yang, Y.; Nunes, F. A.; Berencsi, K.; Furth, E. E.; Gonczol, E.; Wilson, J. M. Cellular immunity to viral antigens limits E1-deleted adenoviruses for gene therapy. *Proc. Natl. Acad. Sci. U.S.A.* **1994**, *91*, 4407−4411.

(34) Knowles, M. R.; Hohneker, K. W.; Zhou, Z.; Olsen, J. C.; Noah, T. L.; Hu, P.-C.; Leigh, M. W.; Engelhardt, J. F.; Edwards, L. J.; Jones, K. R.; et al. A controlled study of adenoviral-vector-mediated gene transfer in the nasal epithelium of patients with cystic fibrosis. *N. Engl. J. Med.* **1995**, *333*, 823−831.

(35) Crystal, R. G.; McElvaney, N. G.; Rosenfeld, M. A.; Chu, C.-S.; Mastrangeli, A.; Hay, J. G.; Brody, S. L.; Jaffe, H. A.; Eissa, N. T.; Danel, C. Administration of an adenovirus containing the human CFTR cDNA to the respiratory tract of individuals with cystic fibrosis. *Nat. Genet.* **1994**, *8*, 42−51.

(36) Hashimoto, T.; Yamaoka, T. Polymericgenecarrier. In *Non-viral gene therapy gene and delivery*; Taira, K., Kataoka, K., Niidome, T., Eds.; Springer: Tokyo, 2005; pp 35−50.
(37) Bhattacharya, S.; Bajaj, A. Recent advances in lipid molecular design. *Curr. Opin. Chem. Biol.* **2005**, *9*, 647−655.
(38) Kumar, M.; Jinturkar, K.; Yadav, M. R.; Misra, A. Gemini Amphiphiles: A Novel Class of Nonviral Gene Delivery Vectors. *Crit. Rev. Ther. Drug Carrier Syst.* **2010**, *27*, 237−278.
(39) Kumar, R.; Santa Chalarca, C. F.; Bockman, M. R.; Bruggen, C. V.; Grimme, C. J.; Dalal, R. J.; Hanson, M. G.; Hexum, J. K.; Reineke, T. M. Polymeric delivery of therapeutic nucleic acids. *Chem. Rev.* **2021**, *121*, 11527.
(40) Muripiti, V.; Rachamalla, H. K.; Banerjee, R.; Patri, S. V. α-Tocopherol-based cationic amphiphiles with a novel pH sensitive hybrid linker for gene delivery. *Org. Biomol. Chem.* **2018**, *16*, 2932−2946.
(41) Gosangi, M.; Ravula, V.; Rapaka, H.; Patri, S. V. α-Tocopherol-anchored gemini lipids with delocalizable cationic head groups: the effect of spacer length on DNA compaction and transfection properties. *Org. Biomol. Chem.* **2021**, *19*, 4565−4576.
(42) Cardoso, A. M.; Morais, C. M.; Cruz, A. R.; Silva, S. G.; do Vale, M. L.; Marques, E. F.; de Lima, M. C. P.; Jurado, A. S. New serine-derived gemini surfactants as gene delivery systems. *Eur. J. Pharm. Biopharm.* **2015**, *89*, 347−356.
(43) Zakharova, L. Y.; Gabdrakhmanov, D. R.; Ibragimova, A. R.; Vasilieva, E. A.; Nizameev, I. R.; Kadirov, M. K.; Ermakova, E. A.; Gogoleva, N. E.; Faizullin, D. A.; Pokrovsky, A. G.; Korobeynikov, V. A.; Cheresiz, S. V.; Zuev, Y. F. Structural, biocomplexation and gene delivery properties of hydroxyethylated gemini surfactants with varied spacer length. *Colloids Surf., B* **2016**, *140*, 269−277.
(44) Yadav, M. R.; Kumar, M.; Murumkar, P. R.; Hazari, P. P.; Mishra, A. K. Gemini Amphiphile-Based Lipoplexes for Efficient Gene Delivery: Synthesis, Formulation Development, Characterization, Gene Transfection, and Biodistribution Studies. *ACS Omega* **2018**, *3*, 11802−11816.
(45) Zana, R.; Xia, J. Geminisurfactants: synthesis, interfacial and solution-phase behavior, and applications; Marcel Dekker Inc.: NewYork, 2004; p *109*.
(46) Ralston, A. W.; Eggenberger, D. N.; Harwood, H. J.; Brow, P. L. D. The Electrical Conductivities of Long-Chain Quaternary Ammonium Chlorides Containing Hydroxyalkyl Groups. *J. Am. Chem. Soc.* **1947**, *69*, 2095−2097.
(47) Choi, J. S.; Lee, E. J.; Jang, H. S.; Park, J. S. New Cationic Liposomes for Gene Transfer into Mammalian Cells with High Efficiency and Low Toxicity. *Bioconjugate Chem.* **2001**, *12*, 108−113.
(48) Wuand, W.; Cseke, L. J. DNA foot printing and gel retardation assay. *Handbook of molecular and cellular methods in biology and medicine*, 2nd ed.; Cseke, L. J.; Peter, B.; Kaufman, P. B.; Podila, G. K.; Tsai, C. J., Eds.; CRC Press, 2003; p 156.
(49) Zuidam, N. J.; Barenholz, Y.; Minsky, A. Chiral DNA packaging in DNA-cationic liposome assemblies. *FEBS Lett.* **1999**, *457*, 419−422.
(50) Zuidam, N. J.; Barenholz, Y. Electrostatic and structural properties of complexes involving plasmid DNA and cationic lipids commonly used for gene delivery1A preliminary report of this study was presented at the 3rd annual conference: Artificial Self-Assembling Systems for Gene Delivery, organized by Cambridge Healthtec Institute, November 17-18, 1996, Coronado, CA.1. *Biochim. Biophys. Acta, Biomembr.* **1998**, *1368*, 115−128.
(51) Simberg, D.; Danino, D.; Talmon, Y.; Minsky, A.; Ferrari, M. E.; Wheeler, C. J.; Barenholz, Y. Phase Behavior, DNA Ordering, and Size Instability of Cationic Lipoplexes. *J. Biol. Chem.* **2001**, *276*, 47453.
(52) Zhang, Z.; Huang, W.; Tang, J.; Wang, E.; Dong, S. Conformational transition of DNA induced by cationic lipid vesicle in acidic solution: spectroscopy investigation. *Biophys. Chem.* **2002**, *97*, 7−16.
(53) Keller, D.; Bustamante, C. Theory of the interaction of light with large inhomogeneous molecular aggregates. II. Psi-type circular dichroism. *J. Chem. Phys.* **1986**, *84*, 2972.
(54) Radler, J. O.; Koltover, I.; Salditt, T.; Safinya, C. R. Structure of DNA-cationic liposome complexes: DNA intercalation in multilamellar membranes in distinct interhelical packing regimes. *Science* **1997**, *275*, 810−814.
(55) Lenssen, K.; Jantscheff, P.; von Kiedrowski, G.; Massing, U. Combinatorial synthesis of new cationic lipids and high-throughput screening of their transfection properties. *ChemBioChem* **2002**, *3*, 852−858.
(56) Ashfaq, R. Radiolabeling, Characterization and Biodistribution study of Cysteine and its derivatives with Tc99m. *J. Nucl. Med.* **2016**, *57*, 1111.
(57) Ralston, A. W.; Eggenberger, D. N.; Harwood, H. J.; Brow, P. L. D. The Electrical Conductivities of Long-Chain Quaternary Ammonium Chlorides Containing Hydroxyalkyl Groups. *J. Am. Chem. Soc.* **1947**, *69*, 2095−2097.
(58) Bombelli, C.; Faggioli, F.; Luciani, P.; Mancini, G.; Sacco, M. G. Efficient transfection of DNA by liposomes formulated with cationic gemini amphiphiles. *J. Med. Chem.* **2005**, *48*, 5378−5382.
(59) Bajaj, A.; Paul, B.; Kondaiah, P.; Bhattacharya, S. Structure−Activity Investigation on the Gene Transfection Properties of Cardiolipin Mimicking Gemini Lipid Analogues. *Bioconjugate Chem.* **2008**, *19*, 1283−1300.
(60) Ma, B.; Zhang, S.; Jiang, H.; Zhao, B.; Hongtao, L. Lipoplex morphologies and their influences on transfection efficiency in gene delivery. *J. Controlled Release* **2007**, *123*, 184−194.
(61) Zhang, Z.; Huang, W.; Tang, J.; Wang, E.; Dong, S. Conformational transition of DNA induced by cationic lipid vesicle in acidic solution: spectroscopy investigation. *Biophys. Chem.* **2002**, *97*, 7−16.
(62) Keller, D.; Bustamante, C. Theory of the interaction of light with large inhomogeneous molecular aggregates. II. Psi-type circular dichroism. *J. Chem. Phys.* **1986**, *84*, 2972.
(63) Srilakshmi, G. V.; Sen, J.; Chaudhuri, A.; Ramadas, Y.; Madhusudhana Rao, N. Anchor-dependent lipofection with non-glycerol based cytofectins containing single 2-hydroxyethyl head groups11IICT Communication No. 4813. *Biochim. Biophys. Acta* **2002**, *1559*, 87−95.
(64) Banerjee, R.; Das, P. K.; Srilakshmi, G. V.; Chaudhuri, A.; Rao, N. M. Novel Series of Non-Glycerol-Based Cationic Transfection Lipids for Use in Liposomal Gene Delivery. *J. Med. Chem.* **1999**, *42*, 4292−4299.
(65) Laxmi, A. A.; Vijayalakshmi, P.; Balagopala Kaimal, T. N.; Chaudhuri, A.; Ramadas, Y.; Rao, N. M. Novel Non-Glycerol-Based Cytofectins with Lactic Acid-Derived Head Groups. *Biochem. Biophys. Res. Commun.* **2001**, *289*, 1057−1062.
(66) Soboleski, M. R.; Oaks, J.; Halford, W. P. Green fluorescent protein is a quantitative reporter of gene expression in individual eukaryotic cells. *FASEB J.* **2005**, *19*, 440−442.
(67) van Meerloo, J.; Kaspers, G. J. L.; Cloos, J. Cell sensitivity assays: the MTT assay. *Methods Mol. Biol.* **2011**, *731*, 237−245.
(68) Sylvester, P. W. Optimization of the tetrazolium dye (MTT) colorimetric assay for cellular growth and viability. *Methods Mol. Biol.* **2011**, *716*, 157−168.
(69) Pathak, A.; Kumar, P.; Chuttani, K.; Jain, S.; Mishra, A. K.; Vyas, S. P.; Gupta, K. C. Gene Expression, Biodistribution, and Pharmacoscintigraphic Evaluation of Chondroitin Sulfate−PEI Nanoconstructs Mediated Tumor Gene Therapy. *ACS Nano* **2009**, *3*, 1493−1505.

https://doi.org/10.1021/acsomega.1c03667
ACS Omega 2021, 6, 33370−33388